

76

**ORNL**  
**OAK RIDGE MASTER COPY**  
**LABORATORY**

operated by  
**UNION CARBIDE CORPORATION**  
for the  
**U.S. ATOMIC ENERGY COMMISSION**



ORNL-TM-169 *gcl*

*15*

WASTE TREATMENT AND DISPOSAL PROGRESS REPORT  
FOR DECEMBER 1961 AND JANUARY 1962

This document has been approved for release  
to the public by:

*David C. Hamlin* *7/29/95*  
\_\_\_\_\_  
Technical Information Officer      Date  
ORNL Site

**NOTICE**

This document contains information of a preliminary nature and was prepared primarily for internal use at the Oak Ridge National Laboratory. It is subject to revision or correction and therefore does not represent a final report. The information is not to be abstracted, reprinted or otherwise given public dissemination without the approval of the ORNL patent branch, Legal and Infor-

LEGAL NOTICE

This report was prepared as an account of Government sponsored work. Neither the United States, nor the Commission, nor any person acting on behalf of the Commission:

A. Makes any warranty or representation, expressed or implied, with respect to the accuracy, completeness, or usefulness of the information contained in this report, or that the use of any information, apparatus, method, or process disclosed in this report may not infringe privately owned rights; or

B. Assumes any liabilities with respect to the use of, or for damages resulting from the use of any information, apparatus, method, or process disclosed in this report.

As used in the above, "person acting on behalf of the Commission" includes any employee or contractor of the Commission, or employee of such contractor, to the extent that such employee or contractor of the Commission, or employee of such contractor prepares, disseminates, or provides access to, any information pursuant to his employment or contract with the Commission, or his employment with such contractor.

ORNL-TM- 169

CHEMICAL TECHNOLOGY DIVISION  
AND  
HEALTH PHYSICS DIVISION

WASTE TREATMENT AND DISPOSAL PROGRESS REPORT  
FOR DECEMBER 1961 AND JANUARY 1962

R. E. Blanco and E. G. Struxness

DATE ISSUED

JUN 15 1962

OAK RIDGE NATIONAL LABORATORY  
Oak Ridge, Tennessee  
Operated by  
UNION CARBIDE CORPORATION  
for the  
U.S. ATOMIC ENERGY COMMISSION

## CONTENTS

	Page
1.0 Introduction	6
2.0 High-Level Waste Calcination	7
2.1 Evaporation-Calcination	7
2.2 Fixation in Glasses	10
2.3 Corrosion	14
3.0 Low-Level Waste Treatment	20
3.1 Pilot Plant	21
3.2 Laboratory Studies	29
4.0 Engineering, Economic and Hazards Evaluation	30
5.0 Disposal in Deep Wells	32
5.1 Disposal by Hydraulic Fracturing	32
5.2 Liquid Injection into Permeable Formations	49
6.0 Disposal in Natural Salt Formations	53
6.1 Field Tests	53
6.2 Laboratory Study of High-Temperature Effects	55
6.3 Plastic Flow Studies	56
7.0 Clinch River Study	56
7.1 Dispersion Studies	56
7.2 Analysis of Clinch River Water and Sediments	58
8.0 Fundamental Studies of Minerals	58
8.1 Dissolution of Calcium from Calcite	62
8.2 Dissolution of Calcium from Rock Phosphate	62
9.0 White Oak Creek Basin Study	64
9.1 Distribution and Transport of Radionuclides in the Bed of Former White Oak Lake	64
9.2 Geologic and Hydrologic Studies	64
10.0 References	67

## ABSTRACT

High-Level Waste Calcination. Energy balance calculations for the Idaho Chemical Processing Plant Pot Calcination Demonstration, on a hypothetical Purex waste, indicate that an 8-in.-dia pot must be used for wastes decayed less than 180 days; a 12-in.-dia one may be used for older wastes. The maximum vapor rates to the fractionator for Purex wastes are approximately 20% greater than those predicted for TBP-25, but the column will operate below flooding at the higher rate.

Equipment is being designed and fabricated for a small scale demonstration of pot calcination in a hot cell at ORNL. The pot will be 4 in. dia and 24 in. high. Synthetic wastes spiked with fission products from Idaho, Hanford, and other hot operations at ORNL will be used for the pot calciner feed solutions. In nonradioactive tests, average overall evaporation-calcination rates for the full scale (90- x 8-in. dia) pot calciner decreased with increased filling (evaporation) time. This is attributed to the formation of higher bulk densities and consequently higher thermal conductivities in the final product. In 11 tests with simulated wastes, Darex, TBP-25, and TBP-25 containing organic residues, batch and continuous flowsheets were demonstrated, with satisfactory control of the continuous evaporator. Filling rates were 8.6 to 19.4 liters/hr averaged over the filling period depending on feed type, concentration, and filling time, with final solid product bulk densities ranging from 0.61 to 1.42 g/cm<sup>3</sup>.

The product of semicontinuous evaporation and fixation of simulated TBP-25 waste to form a lead phosphate glass (additives: 2 moles of NaH<sub>2</sub>PO<sub>2</sub> and 0.25 mole of PbO per liter) in a 24- x 4-in.-dia stainless steel pot had a density of 2.9 g/ml and a volume about 1/8 that of the concentrated (1.72 M Al) waste solution. Ruthenium volatility was as low as 3% during processing. The thermal conductivity of the glass varied from 1.05 Btu/hr.ft.<sup>2</sup>°F at 300°F to 1.60 Btu/hr.ft.<sup>2</sup>°F at 1050°F; the temperature coefficient was positive and nonlinear with temperature, indicating an amorphous solid.

Corrosion of stainless steel "pots" used for the evaporation-fixation process was maximum in every case during the period when the last acid and water were being driven off at 850-1000°C. Overall corrosion rates for evaporation-fixation of Purex and TBP-25 wastes were about 5-11 mils/mo in a 24-hr batch process, about 1.4 mil/mo of which was attributable to air oxidation. When glass-making additives were present, rates increased to 42 mils/mo for the TBP-25 lead-phosphate glass at 920°C and to 145 mils/mo for a Purex borophosphate glass at 900°C. Release of SO<sub>3</sub> from the Purex waste is responsible for highly aggressive intergranular attack, which can be catastrophic at temperatures above 900°C, the critical temperature depending on the melt composition. Titanium was corroded at a maximum rate of about 2 mils/mo in evaporator-calciner environments vs about 10 mils/mo for LCNA and 11.2 mils/mo for Hastelloy F.

Low-Level Waste Treatment. In four continuous runs in the waste treatment pilot plant, ORNL low-activity waste was decontaminated from Sr-90 and Cs-137 by factors of >2000 and >246, respectively. The plant effluent contained <1.5% of the current MPC<sub>w</sub> values for these isotopes for a 168-hr week. Run times were from 71 to 100 hr of continuous operation, with the use of 1800-2100 resin bed volumes. Equipment performance was good except for the rotary-drum vacuum filter, which was replaced by a plate-and-frame pressure filter modified to meet radiation protection requirements.

In laboratory-scale studies cobalt and ruthenium removal from the pilot plant effluent was improved by addition of an anion exchange column to the system and BO-4 grade vermiculite was plugged by small amounts of solids in the stream. Nalco analytical reagents were satisfactory, 1 ppm accuracy, for pilot plant control analyses.

Engineering, Economic, and Hazards Evaluation. Space requirements to dissipate the fission product heat in the waste from a 56,000-Mw(th) nuclear power economy were calculated for cylinders of calcined waste buried vertically in the floors of rooms in salt media. Spacings between cylinders ranged from 36 ft for acidic Purex in 24-in.-dia cylinders at the minimum burial age to 1 ft for reacidified Thorex in 6-in.-dia cylinders at 30 years age. Area requirements were calculated from the cylinder production rate and spacing requirements. Net area requirements calculated for Purex wastes in acidic and reacidified forms in 6-, 12-, and 24-in.-dia vessels range from 20 acres/year after 0.65 year to about 2 acres/year at 30 years age at burial. Corresponding areas for Thorex wastes are 10 and 0.7 acres/year. Calculations were made also for an acidic Thorex glass in 6-in.-dia vessels. The primary effects of the form of the waste (acidified, reacidified, glass) and vessel diameter are to limit the minimum burial age, although area requirements may be affected by factors of 2-3 by waste form and vessel size near the minimum burial ages.

Disposal in Deep Wells. Two fracturing experiments showed that structurally conformable fractures can be formed by hydraulic fracturing in the Conasauga shale at Oak Ridge. In the second experiment, two batches of a tagged grout mixture (91,567 gal in the first batch and 132,770 gal in the second) were injected into the same well at depths of 934 and 694 ft, respectively. Average injection pressures ranged from 1650 psi at 138 gpm in the first (lower) injection to 2000 psi at 200 gpm in the second (upper) injection, substantially higher than the rule-of-thumb value of 1 psi per foot of depth. Subsequent test drilling suggests that the lower grout sheet is ~240,000 ft<sup>2</sup> in area, oriented north and south, and that the upper grout sheet has an area of about 245,000 ft<sup>2</sup> in the east-northeast direction. The average thickness of the lower grout sheet is 0.01 ft and of the upper, 0.03 ft.

Sodium-calcium-strontium exchange was studied with Richfield sand as the sorbent. Strontium is sorbed selectively over calcium by a factor of ~1.1, while the selectivity of calcium sorption over sodium, at pH 7, was ~50 g/ml. The normalized strontium breakthrough curves correspond to the anion breakthrough curves, indicating that strontium breakthrough can be predicted from the solution dispersion in the column.

Disposal in Natural Salt Formations. Laboratory experiments showed that large pieces of salt heated to 260 to 280°C are shattered with some violence, accompanied by a release of steam. To evaluate the effect of high temperature on rock salt in place, a length of 6-5/8-in.-o.d. pipe, electrically heated to simulate a container of high-activity radioactive solids, was placed in a 7-7/8-in.-dia drilled hole in the floor of the Hutchinson mine. After 3.5 days' heating, the experiment was terminated because of the presence of water and recrystallized salt in the annulus surrounding the container. Temperatures as high as 127°C (106°C rise) were measured at 9.6 in. from the center of the heater. The surface temperature of the hole, extrapolated from this value, was about 200°C.

Clinch River Studies. During a period of 20,000 cfs flow in the Clinch River, with the level of Watts Bar Reservoir at 735 ft above mean sea level, the time of travel of Au-198 tracer from the mouth of White Oak Creek to Centers Ferry was 9.3 hr, about 10% less than predicted from computation of the mean velocity.

The effect of power releases from Norris Reservoir (the flow in the Clinch River varied from 1700 to 7700 cfs in 24 hr) on the level of radioactivity at a section 15.3 miles downstream from White Oak Creek was found to be insignificant. The deviation in radionuclide concentration during the period was less than 10% of the average concentration.

In 1963, power releases from Melton Hill Reservoir may cause daily variations in the flow of the Clinch River, from 0 to 23,000 cfs. At the maximum release rate, the level of backwater from Clinch River into White Oak Creek will be 3.5 ft above present summer levels. Unless the control gate settings at White Oak Dam are changed, the backwater will flow into White Oak Lake. If the gate levels are raised to prevent inflow from the river, the inflow from the creek to White Oak Lake will raise the lake levels.

Fundamental Studies of Minerals. In studies on the role of sodium nitrate in removing strontium from calcite and rock phosphate columns, the calcium dissolved by 1 M NaNO<sub>3</sub> was 1.1 mM, almost four times the solubility of calcite in water. The dissolution of calcite was the same in three successive leaches, but the amount of calcium in solution contacted with rock phosphate decreased in each of three successive leaches. Equilibrium was reached within 15 min for calcite particles up to 0.5 mm dia; rock phosphate samples showed increasing calcium in the solution contacted with increasing contact time up to 5 hr.

White Oak Creek Basin Study. Water-level measurements, taken in observation wells in the former bed of White Oak Lake, indicate that the depth to ground water varies from <1 ft to 4 ft below the land surface. Water-contour maps show that the general direction of ground-water movement is normal to the flow of White Oak Creek in the lower lake bed, but the pattern in the upper portion is influenced by stream flow from the intermediate-level waste seepage pit area.

## 1.0 INTRODUCTION

This report is the fifth in a series\* of bimonthly reports on progress in the ORNL development program, the objective of which is to develop and demonstrate on a pilot plant scale integrated processes for treatment and ultimate disposal of radioactive wastes resulting from reactor operations and reactor fuel processing in the forthcoming nuclear power industry. The wastes of concern include those of high, intermediate, and low levels of radioactivity in liquid, solid, or gaseous states.

Principal current emphasis is on high- and low-activity liquid wastes. Under the integrated plan, low-activity wastes, consisting of very dilute salt solutions such as cooling water and canal water, would be treated by scavenging and ion exchange processes to remove radioactive constituents and the water discharged to the environment. The retained waste solids or slurries would be combined with the high-level wastes. Alternatively, the retained solids or the untreated waste could be discharged to the environment in deep geologic formations. The high-activity wastes would be stored at their sites of origin for economic periods to allow for radioactive decay and artificial cooling.

Two methods are being investigated for permanent disposal of high-activity wastes. One approach is conversion of the liquids to solids by high-temperature "pot" calcination or fixation in the final storage container (pot) itself and storage in a permanently dry environment such as a salt mine. This is undoubtedly the safest method since complete control of radioactivity can be ensured within present technology during treatment, shipping, and storage. Another approach is disposal of the liquid directly into sealed or vented salt cavities. Research and development work is planned to determine the relative feasibility, safety, and economics of these methods, although the major effort will be placed on conversion to solids and final storage as solids.

Tank storage or high-temperature calcination of intermediate-activity wastes may be unattractive because of their large volumes. Consequently, other disposal methods will be studied. One method, e.g., addition of solidifying agents prior to direct disposal into impermeable shale by hydrofracturing, is under investigation at present. Particular attention is given to the engineering design and construction of an experimental fracturing plant to dispose of ORNL intermediate-activity wastes by this method if proved feasible.

Environmental research on the Clinch River, motivated by the need for safe and realistic permissible limits of waste releases, is included in this program. The objective is to obtain a detailed characterization of fission product distribution,

---

\* Previous: ORNL-CF-61-7-3, ORNL-TM-15, ORNL-TM-49, and ORNL-TM-133.

transport, and accumulation in the physical, chemical, and biological segments of the environment.

## 2.0 HIGH-LEVEL WASTE CALCINATION

The pot calcination process for converting high-activity-level wastes to solids is being studied on both a laboratory and engineering scale to provide design information for construction of a pilot plant. Development work has been with synthetic Purex, Darex, and TBP-25 wastes containing millicurie amounts of ruthenium but has not been demonstrated on actual high-activity-level wastes. A general flowsheet was shown previously (1).

### 2.1 Evaporation-Calcination

#### 2.1.1 Pilot Plant Flowsheet Calculations (E. J. Frederick, J. O. Blomeke, J. M. Holmes, V. R. Young)

Chemical flowsheets are being prepared for each type of waste to be processed in the Pot Calciner Pilot Plant at ICPP. Maximum and minimum heat and material flows at each point in the process are being computed for Purex, TBP-25, and Darex wastes for use in design. In a hypothetical case considered, 1 ton of low enriched uranium metal is irradiated and processed by the Purex method. The total decay time of the waste, from reactor discharge of the fuel to waste processing, is 180 days. Heat transfer calculations indicate that in order to prevent a temperature  $>900^{\circ}\text{C}$  at the center of the pot containing the calcined cake, an 8-in.-dia pot would be required. Since the probability of processing wastes aged greater than 180 days appears realistic, a flowsheet was prepared also for 12-in.-dia pots.

Analysis of data from Purex Runs R-42 through R-46 showed the limits for batch and continuous flowsheets. Heat balances across the calciner condenser showed a maximum vapor flow from the calciner of 164 lb/hr. Assuming ideal gas conditions, a corresponding vapor velocity in the pot of 3.0 ft/sec is calculated for an 8-in.-dia pot. The excess capacity that will be built into the furnace to be installed as part of the process at the ICPP permits extending this vapor rate to a 12-in.-dia pot with a maximum predicted flow of approximately 240 lb/hr. Operation of the evaporator at maximum boilup would give an overhead vapor flow of 1360 lb/hr from the evaporator to the fractionator. This value is approximately 20% higher than the maximum rate calculated for the TBP-25 waste, which had been considered design-limiting. Pressure drop calculations in the vapor line from the evaporator based on a flow of 1360 lb/hr show a loss of approximately 0.08 in. water per foot of pipe length. Pressure drop in the distillation column at this same flow rate is approximately 1.08 in. water per foot of column height at a superficial vapor velocity of 7.21 ft/sec. Flooding velocity for these same conditions is 10.4 ft/sec.

### 2.1.2 Design of Experimental Hot Cell (H. O. Weeren, J. O. Blomeke)

Design of the equipment for study of evaporation and calcination of actual high-activity waste in a cell is essentially complete (Fig. 2.1). Waste solution will be charged from the carrier on the roof of the cell, at the right of the drawing, to the transfer tank and to the feed tank and thence to the calciner pot by air lifts. The vapor from the calciner pot will go through a jacketed section of line to the condenser, then to a scrubber, and will be recycled through a gas pump to the calciner pot. Calcined wastes will be removed to the carrier on the roof of the cell, at the left. The evaporator pot, sampler lines, vent lines, waste discharge lines, and service lines are not shown in this drawing. The pot will be 4 in. dia and 24 in. high.

A second calcining furnace will be installed to serve as a spare in case the furnace fails. The furnaces will be mounted on a small dolly so that the first can be moved out of the way and the second moved into position, both remotely. A small air blower mounted on the furnace dolly will circulate cell air through the annular area between the furnace and the pot, the flow being directed to either furnace by a flapper valve.

Several calcination runs with synthetic waste solution spiked with fission products obtained from other hot cell operations are planned. The fission product solution produced in hot cell experiments will be stored in 2-liter stainless steel cans, which will be transferred to the cell through the sample chute and emptied into the feed tank when fission products are needed in a calcination experiment.

### 2.1.3 Engineering-scale Nonradioactive Tests (J. C. Suddath, C. W. Hancher, L. J. King)

Eleven engineering-scale tests, 8-in.-dia x 90-in.-high pot, were completed with synthetic TBP-25 and Darex wastes in the batch and continuous evaporator systems. The evaporator and its control system were modified to increase the stability of operation. Modifications included changing the natural circulation loop of the evaporator to give easier circulation, cascade of the density-steam controller so that the density controller calls for a steam pressure in the steam chest and the second controller regulates the steam supply valve to give the desired pressure, and installation of a conductivity cell on the evaporator condensate to indicate acid concentration.

Feed Rates. With TBP-25 waste, the average feed rate varied with the fraction of pot filled (bulk density) at the end of the tests, from 19.4 liters/hr at a density of 0.6 g/cm<sup>3</sup> to 11.6 liters/hr at a density of 0.8 g/cm<sup>3</sup>. Increasing the operating liquid level ~6 in. gave a rate of 17.6 liters/hr with a density of 0.83 g/cm<sup>3</sup>. The addition of organic, 0.01 M TBP, to the feed decreased the average rates and density ~50%. With Darex waste average feed rates were 8.6 to 16.5 liters/hr and bulk densities were 0.63 to 1.42 g/cm<sup>3</sup>. Average feed rates were based on the filling

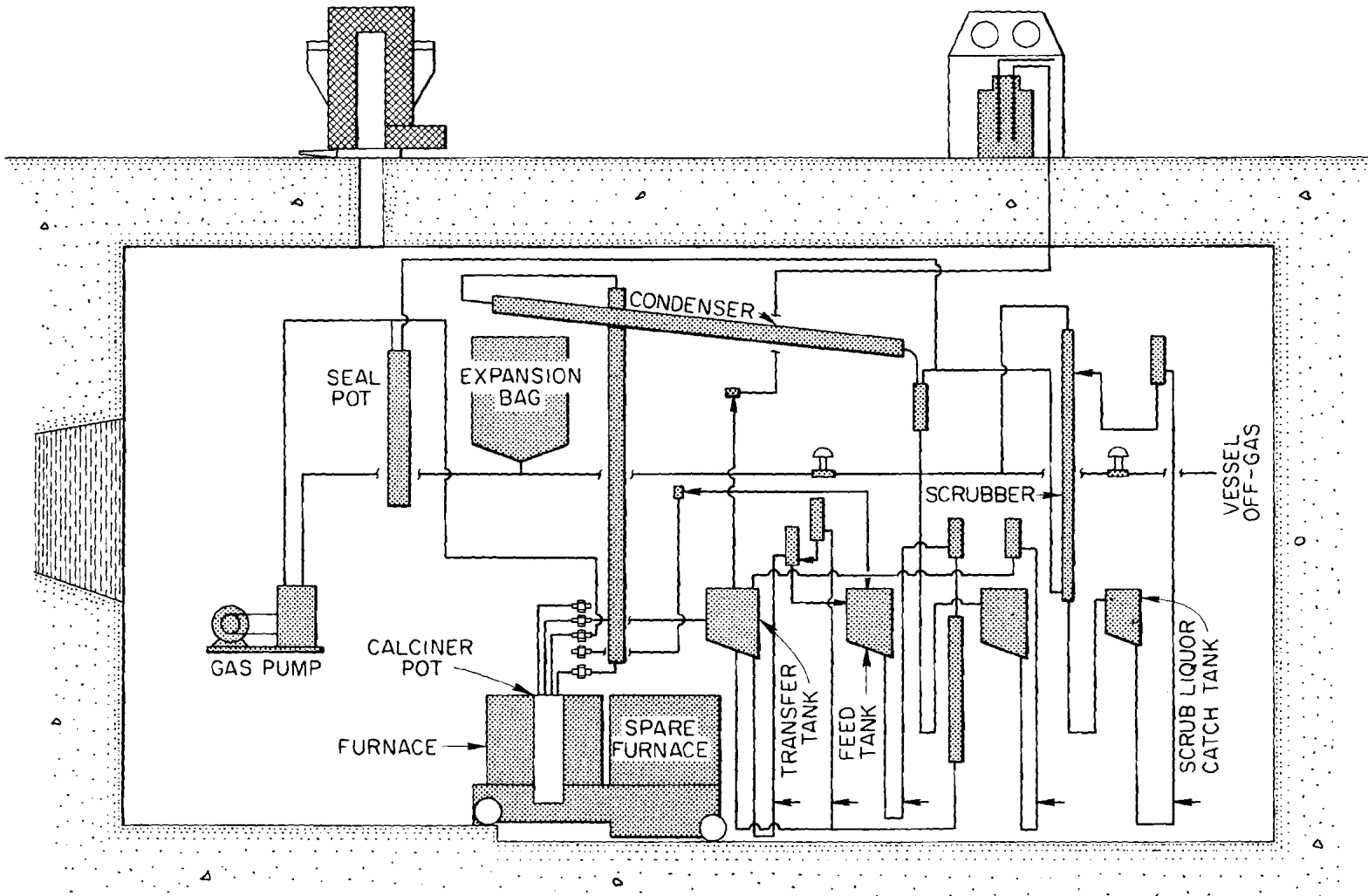


Fig. 2.1 Equipment in hot cell for pot calcination experiment.

time only (Table 2.1), since the calcination time depends on activity level, and change-out time on the mechanical design.

In one test (R-64) with TBP-25 waste, in which filling was stopped, the solids were calcined, and then another filling operation and calcination were made in the same pot, the overall filling rate was 11.6 liters/hr.

Mercury Build-up. In two successive tests with no draining or flushing of the evaporator, 23% of the mercury remained in the evaporator at the end of the first test, and the calciner off-gas line plugged with mercury oxides during the second. A mercury trap to prevent this has been fabricated.

## 2.2 Fixation in Glasses (H. W. Godbee, W. E. Clark)

A second semicontinuous evaporation, calcination, and heating to 1000°C of a simulated TBP-25 waste solution\* plus selected additives gave a product with a density of approximately 2.9 g/ml, representing about 1 vol of glass per 8 vol of concentrated waste. This result agrees with that of the first semicontinuous experiment (2) and compares favorably with a previous batch experiment (3) in which the product density was 2.84 g/ml and 1 vol of glass represented 8.1 vol of waste. Additives per liter of waste were 2.0 moles of  $\text{NaH}_2\text{PO}_2$  to control ruthenium volatility and to serve as a source of phosphate for glass formation plus 0.25 mole of  $\text{PbO}$  to lower the softening point of the product.

The experiment was performed in previously described equipment (Fig. 6.2 in Ref. 4), consisting of a 24- x 4-in.-dia stainless steel pot in a 9-kw furnace, a downdraft condenser, packed absorber column, polyethylene expansion bag, and off-gas jet. This experiment differed from the first in that the off-gases were not recycled but jetted to the plant off-gas. An all-welded can was used to eliminate air leakage to the can and thus minimize volatilization of ruthenium. Feed was pumped to the pot at ~50 ml/min, with the liquid level in the pot gradually rising from about 6 in. above the bottom to about 4 in. from the top. Heater controls were set to give a maximum pot wall temperature of ~1000°C throughout the run, although this temperature was attained in a given zone only after solidification and melting had occurred. After melting begins, there are three zones in the pot: molten glass, calcining solids, and evaporating liquid. This method of operation has given the smoothest, most reproducible performance of equipment thus far.

---

\* 1.72 M  $\text{Al}^{3+}$ , 0.16 mg/ml  $\text{Fe}^{3+}$ , 4.02 mg/ml  $\text{Hg}^{2+}$ , 2.4 mg/ml  $\text{Na}^+$ , 0.05 M  $\text{NH}_4^+$ , 1.26 M  $\text{H}^+$ , 0.2 mg/ml Ru, 160 ppm  $\text{Cl}^-$ , 6.6 M  $\text{NO}_3^-$ , 1.32 g/ml; 106 gal/kg U-235 processed.

Table 2.1 Results of Tests R-49 Through R-64<sup>a</sup>

Run No.	Feed Type	Avg Feed Rate (liters/hr)	Evaporator Concentration Factor <sup>b</sup>	Water to Feed Vol Ratio	Off-gas <sup>c</sup> to Feed Ratio (ft <sup>3</sup> /liter)	NO <sub>3</sub> in Solids (wt %)	Solids <sup>d</sup> Bulk Density (g/cm <sup>3</sup> )	Total Feed Vol (liters)
R-49	TBP-25	17.6	1.08 - 0.70	2.6	1.9	6.6-0.36	0.83	478
R-50	TBP-25 <sup>e</sup>	11.5	1.30 - 0.71	2.4	2.4	4.1-0.08	0.52	346
R-51 <sup>f</sup>	TBP-25 <sup>e</sup>	7.0	1.35 - 1.15	2.5	3.2	6.0-0.08	0.59	308
R-52 <sup>f</sup>	TBP-25 <sup>e</sup>	9.8	1.02 - 0.93	2.3	2.4	0.2-0.06	0.44	440
R-54	TBP-25	17.2	1.37 - 0.95	2.7	1.8	0.8-0.1	0.65	428
R-55	TBP-25	19.4	2.00 - 0.90	3.5	1.4	0.6-0.1	0.63	468
R-62	TBP-25	16.8	1.43 - 0.74	4.5	1.0	2.0-0.10	0.63	446
R-63	TBP-25	16.3	1.22 - 0.87	2.3	0.9	2.0-0.20	0.61	421
R-64	TBP-25	11.6	1.1 - 0.63	2.1	1.2	0.2-0.002	0.80	560
R-59 <sup>f</sup>	TBP-25 <sup>e</sup>	12.4	1.0	0	1.3	1.0-0.07	0.61	397
R-56	Darex	13.6	1.24 - 0.71	4.1	1.4	0.1-0.02	0.86	383
R-57	Darex	8.9	1.47 - 0.79	3.2	2.2	0.5-0.01	1.40	641
R-58	Darex	16.5	1.69 - 1.38	3.0	0.8	1.0-0.2	1.42	576
R-60 <sup>f</sup>	Darex	8.6	1.09 - 0.65	5.5	1.8	2.0-0.10	1.29	336
R-61 <sup>f</sup>	Darex	10.6	1.0 - 0.82	3.8	-	1.0-0.02	1.13	307

<sup>a</sup>First four runs partially reported in TM-133.

<sup>b</sup>Ratio of concentrations during feeding.

<sup>c</sup>Off-gas volume includes 10-20 ft<sup>3</sup>/hr system inleakage.

<sup>d</sup>Total weight of solids averaged over 60 liter pot volume.

<sup>e</sup>Organic added to feed, 0.01 M TBP.

<sup>f</sup>Batch tests.

Table 2.2 Chemical Compositions of Simulated Waste Solutions Investigated in Evaporation-Fixation Corrosion Studies

Component	Simulated Waste Solution Composition (M)					TBP-25
	Formaldehyde-Treated Purex <sup>a</sup>	Purex <sup>a</sup>	Purex and Additive			
			No. 1	No. 2	No. 3	
H <sup>+</sup>	0.3	5.6				1.3
NO <sub>3</sub> <sup>-</sup>	1.2	6.1				6.6
SO <sub>4</sub> <sup>=</sup>	2.0	1.0				---
Na <sup>+</sup>	1.2	0.6				---
Al <sup>+3</sup>	0.2	0.1				1.72
Fe <sup>+3</sup>	1.0	0.5				~ 0.003
Cr <sup>+3</sup>	0.02	0.01				---
Ni <sup>+2</sup>	0.02	0.01				---
Hg <sup>+2</sup>	---	---				0.02
Ru	0.004	0.002				0.0003
Na <sub>2</sub> B <sub>4</sub> O <sub>7</sub>			0.13	0.344	0.086	
NaH <sub>2</sub> PO <sub>4</sub>			0.76			
NaH <sub>2</sub> PO <sub>2</sub>						2.0
H <sub>3</sub> PO <sub>2</sub>			0.76	1.52	1.52	
MgO				0.80	0.80	
Ca(OH) <sub>2</sub>			1.1			
NaOH			0.22	1.32	1.49	
PbO						0.25

<sup>a</sup>Data have not been obtained for Purex waste without addition of either formaldehyde or fluxing agents. Corrosion should correspond closely to that in the formaldehyde-treated waste.

Ruthenium Volatility. Ruthenium determinations by neutron activation showed 13.7, 0.3, and 0.1% of the original ruthenium in the condensate, liquid from the packed absorber, and the liquid used in the off-gas jet, respectively. Ruthenium in the condensate decreased to 3% of the original as processing was continued, the early high value probably being due to release of ruthenium contamination of the equipment from previous use. Previous results of semicontinuous experiments (2) with this mixture showed a distribution of 22.7, 1.4, and 0.3% of the original ruthenium. Neither experiment agrees with a previous batch experiment (3) with the same mixture containing Ru-106 tracer, where only 0.68% of the original ruthenium was in the condensate and 0.03% or less in the off-gas scrub liquid. The differences appear to be caused by air leakage into the semicontinuous system and by the washing of ruthenium from previous experiments out of the equipment by the condensate. There was definitely air leakage into the equipment during the first semicontinuous experiment (2). In the second experiment, carried out in an all welded, leak-tested pot, ruthenium in the condensate decreased with time from 3.9 to 1.1  $\mu\text{g}/\text{ml}$ , as would be expected from equipment washout. The next semicontinuous experiment will be made with radioactive ruthenium, and the equipment will be leak tested and flushed with NO in order to determine the true ruthenium volatility from the evaporation-fixation process.

Thermal Conductivity. Waste storage conditions must provide for the dissipation of heat generated by the radioactive decay of unstable isotopes to preclude the attainment of a temperature detrimental to the waste, its container, or the surrounding medium. Calculations (5) have shown that a thermal conductivity,  $k$ , of 0.1 Btu/hr-ft. $^{\circ}\text{F}$  is probably high enough for storage of calcined wastes.

The  $k$  values for a phosphate-lead glass incorporating TBP-25 waste oxides, measured in situ, varied from about 1.05 Btu/hr-ft. $^{\circ}\text{F}$  at 300 $^{\circ}\text{F}$  to about 1.60 Btu/hr-ft. $^{\circ}\text{F}$  at 1050 $^{\circ}\text{F}$  (Fig. 2.2). The glass had a positive temperature coefficient of thermal conductivity, a characteristic of amorphous solids and powders, but the variation of  $k$  was nonlinear, a characteristic of amorphous solids but not of powders.

The glass, density 2.9 g/ml, was prepared by semicontinuous evaporation, calcination, and melting of a TBP-25 waste made 2 M in sodium hypophosphite and 0.25 M in lead oxide. Thermal conductivity was determined by a steady-state method using radial heat flow in a hollow cylinder (6) of 1 in. i.d., 4 in. o.d., and 24 in. long. The glass was formed with thermocouples spaced radially throughout it and with a 1-in.-dia stainless steel tube down the center. When a heater was inserted, down the 1 in. tube,  $k$  could be measured without disturbing the glass. The thermal conductivity was calculated by integrating Fourier's law for heat flow in a cylinder (6). The variation with temperature should not be extrapolated to higher temperatures since the phosphate-lead glass begins to soften at about 1100 $^{\circ}\text{F}$  (600 $^{\circ}\text{C}$ ).\*

\*Although the initial softening point of the glass as formed by evaporation, calcination, and melting is about 900 $^{\circ}\text{C}$ , the softening point of the glass after being formed is about 600 $^{\circ}\text{C}$ .

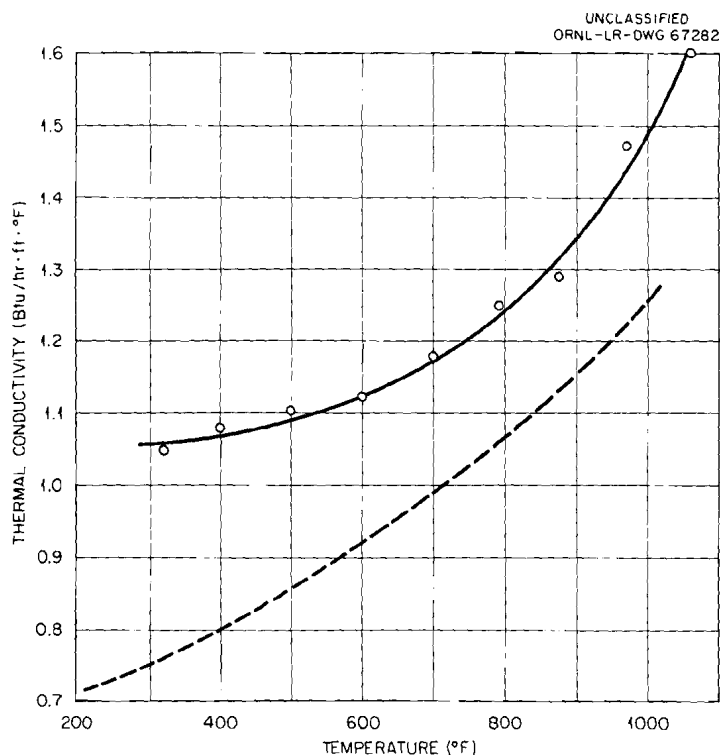


Fig. 2.2 Thermal conductivity of phosphate-lead glass incorporating TBP-25 waste oxides (solid line) and of soda-lime-silica glass (dashed line) (7) as a function of temperature. Composition of phosphate lead glass, wt %: 25.0  $Al_2O_3$ , 18.6  $Na_2O$ , 40.5  $P_2O_5$ , 15.9  $PbO$ , 0.06  $Fe_2O_3$ , 0.01  $RuO_2$ .

Since the liquid state represents a more disordered state, the thermal conductivity should be somewhat lower after the glass softens. Measurements now in progress will show the variation of  $k$  with temperature after softening of the glass.

### 2.3 Corrosion (W. E. Clark, L. Rice,\* D. N. Hess\*)

In the evaporation and fixation in solid form of high-activity radioactive waste, corrosion both of the condenser and off-gas system and of the product container must be considered. The corrosion of a given material varies considerably from one type of waste to another and with operating temperature. Since storage of high-activity waste in reasonably large containers requires a product and a container with fairly good thermal conductivity, stainless steel is considered for the fixation pot, the oxidation of which limits the fixation temperature to about 1100°C. The overhead system (condensers and off-gas lines) presents in many respects a more difficult corrosion problem than the waste pot since the former must be used over and over while the latter is subjected to aggressive corrosion over only one fixation cycle. Also, the effect of small

---

\*Reactor Chemistry Division

amounts of volatile materials such as the halogens and ruthenium in the presence of varying amounts of nitric and sulfuric acids is difficult to assess.

The results of corrosion tests indicated that type 304L stainless steel will be a satisfactory material of construction for waste calcination pots. Corrosion rates for a 24-hr evaporation-fixation cycle to 900°C varied from 5.1 mils/mo for TBP-25 waste to 80 mils/mo for Purex waste with fluxing agents added. Titanium was the most satisfactory material tested in off-gas and condenser environments, with a maximum rate of ~2 mils/mo in refluxing 15 M HNO<sub>3</sub>-1 M H<sub>2</sub>SO<sub>4</sub>.

Experimental Method. For the tests, welded specimens of stainless steel ~6 by 1/2 by 1/4 in. were placed in a Vycor tube containing synthetic waste solution of one of the compositions expected in the evaporation-calcination cycle. The volume of solution was such that an ~3-in. length of each specimen was above the solution-vapor interface. The Vycor tube was inserted in a type 304L stainless steel vessel and a condenser system was attached to the vessel, which was then placed in a vertical-tube furnace. The vessel was slowly heated to ~110°C, at which temperature distillation of the volatile components started. When the distillation rate began to decrease, the vessel temperature was raised to ~250°C and held there until the distillation rate again began to decrease. This procedure was repeated until the vessel reached the desired temperature (900-1000°C), where it was maintained for the remainder of the test.

### 2.3.1 Purex Waste

In two 24-hr tests with formaldehyde-treated synthetic Purex waste solutions, the corrosion rate of welded specimens of type 304L stainless steel was 6.7 and 7.9 mils/mo (Table 2.3). A hard, yellow film that could not be removed by the normal brushing procedure formed over the entire specimen in both cases, but there was no serious localized attack. The corrosion rate after the calcination was completed was calculated to be 3.6 mils/mo from the results of 123 hr heating to 900°C of a specimen with ~100 g of the residue from the evaporation and calcination at 1000°C of synthetic Purex waste. There was no localized attack. These results indicate that most of the observed corrosion occurs during the initial 24 hr.

Welded type 304L specimens were similarly exposed to Purex solution containing glass-making additives except that in most cases a type 304 stainless steel liner was used instead of the Vycor tube because the latter became devitrified during the high-temperature part of the fixation cycle. Overall corrosion rates of 120 and 145 mils/mo were calculated from the results of 24-hr tests. Both specimens were intergranularly attacked uniformly over the entire surface. Overall corrosion rates were 80 and 57 mils/mo, respectively, again with intergranular attack in two 78-hr tests. In the first test the system was brought to ~900°C and held there for 78 hr. In the second, the system was held at 110°C until distillation ceased, when the system was cooled and the specimen examined and weighed. No measurable corrosion had occurred. The specimen was placed in the system again, the temperature was raised to

Table 2.3 Summary of Corrosion of Stainless Steels in Evaporation-Fixation Tests of Simulated High-Level Waste Solutions

Material	Environment	Max Temp (°C)	Exposure Time (hr) <sup>a</sup>	Overall Corrosion Rate (mils/mo)
304L	Air	~900	24	1.4
304L	Purex, formaldehyde treated	~900	24	6.7
304L	Purex, formaldehyde treated	~900	24	7.9
304L	Purex solids (after calcination to ~1000°C)	~900	123	3.6
304L	Purex + additives	~900	24	120 <sup>b</sup>
304L	Purex + additives	~900	24	145 <sup>b</sup>
304L	Purex + additives	~900	78	80 <sup>b</sup>
304L	Purex + additives	~850	1	~0
		~950	2	1330 <sup>c</sup>
		~950	75	19
304L	TBP-25	~900	24	5.10
347	TBP-25	~900	24	10.5
304L	TBP-25	~900	168	1.59
347	TBP-25	~900	168	1.93
304L	TBP-25 + additives	920	19	42.2
304L	TBP-25 + additives	910	345	5.4

<sup>a</sup>Time at maximum temperature listed.

<sup>b</sup>Intergranular attack noted.

<sup>c</sup>Highly aggressive localized attack (intergranular).

~850°C for 1 hr, and the system was again cooled. The specimen still showed no corrosion. But when the specimen was again placed in the system which was heated to ~950°C and held there 2 hr and then cooled, the specimen showed intergranular corrosion over the entire surface and a corrosion rate of 1330 mils/mo was calculated. The specimen was again placed in the system, which was heated to 950°C again and held there for 75 hr. The corrosion rate calculated for the 75-hr period was 19 mils/mo. The overall rate for the whole test was calculated to be 57 mils/mo. This second experiment indicates that essentially all the observed corrosion occurred during the first 2-4 hr at the temperature required to remove the last of the acid and water from the system.

Nature of Attack. The nature of the corrosion attack on the inner and outer surfaces (vapor) of a type 304L stainless steel calcination vessel (liner) is shown in Fig. 2.3, which is a photomicrograph of the metal ~4 in. from the bottom of the vessel, i.e., ~1.5 in. above the initial solution-vapor interface. The top of the photomicrograph shows the type of attack to be expected between the melt and the container material. Although it is not apparent in the figure, this attack is intergranular. The lower part of the photomicrograph shows that serious intergranular corrosion may occur in the vapor.

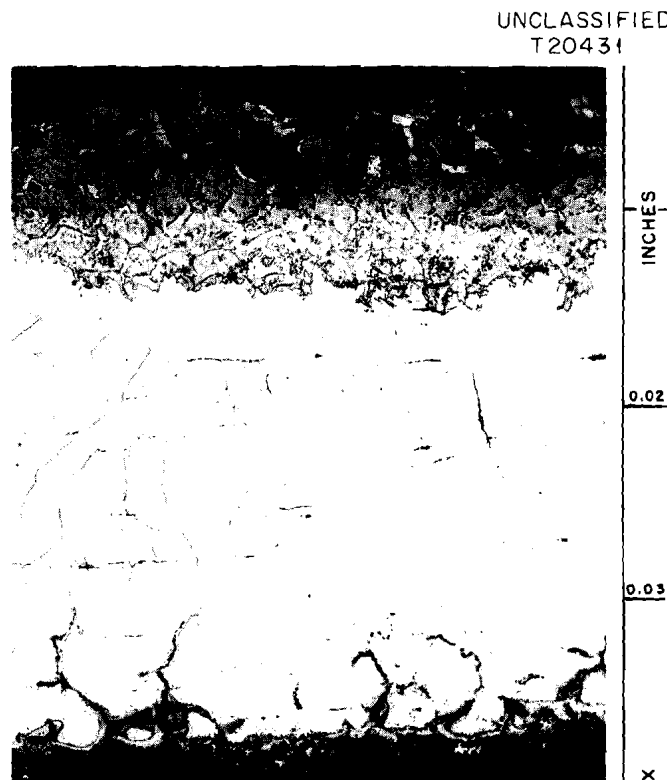


Fig. 2.3 Intergranular attack on a type 304L stainless steel calcination vessel after 24-hr exposure to synthetic Purex waste during a single evaporation-fixation cycle.

An occasional more aggressive localized attack observed during calcination of Purex waste containing glass-making additives was thought to be due to release of  $\text{SO}_3$  and/or  $\text{H}_2\text{SO}_4$  at temperature above  $900^\circ\text{C}$ . This hypothesis was confirmed by thermograms made from the solid products obtained from evaporation and fixation of simulated Purex waste in magnesium\* borophosphate "glasses" of two different compositions (Table 2.2). The thermograms also emphasize the importance of close temperature control during fixation of high-sulfate Purex waste and the necessity of determining the effect of any additives on the temperature of  $\text{SO}_3$  evolution.

The first thermogram (Fig. 2.4) was made from the product formed by the addition of borax, phosphorous acid,  $\text{MgO}$ , and  $\text{NaOH}$  to the waste to final molarities of  $\sim 0.34$ ,  $1.52$ ,  $0.80$ , and  $1.34$ , respectively. The softening point of the product was  $\sim 825^\circ\text{C}$ . Very little weight loss was observed below  $900^\circ\text{C}$ , but increasing the temperature above  $900^\circ\text{C}$  resulted in volatilization of a material that was identified by odor as  $\text{SO}_3$ . Above  $1200^\circ\text{C}$  the melt formed tended to "crawl" out of the thermobalance bucket; therefore the weight loss curve was extrapolated to approximate the curve expected from the loss of a single component due to thermal decomposition. Assuming the material lost to be  $\text{SO}_3$ , the theoretical weight loss is 22.4% of the original specimen weight vs 21.89% obtained from the extrapolated curve.

A second thermogram (Fig. 2.5) was made from the solid material obtained from evaporation of a Purex waste solution containing additives to the extent of  $0.086\text{ M}$  borax,  $1.52\text{ M}$  phosphorous acid,  $0.80\text{ M}$   $\text{MgO}$ , and  $1.49\text{ M}$   $\text{NaOH}$ . The temperature was raised slowly to  $520^\circ\text{C}$  and then held constant until denitration was essentially complete. Further increase in temperature caused only a small weight loss until the temperature approached  $1000^\circ\text{C}$ , when loss of  $\text{SO}_3$  started.

Condenser System. Titanium 45A was far more satisfactory than Hastelloy F, LCNA,\*\* or 347 stainless steel in resistance to the condensate expected from the initial and final stages of evaporation and calcination (without additives) of high-sulfate Purex waste solutions, as well as to an estimated "average" condensate from such a process (Tables 2.5-2.7). The maximum rate for titanium 45A was 2.01 mils/mo for 1145 hr exposure in the solution phase of refluxing  $15\text{ M}$   $\text{HNO}_3$ - $1\text{ M}$   $\text{H}_2\text{SO}_4$  (Table 2.7). There was some local attack in the heat-affected zone near the weldments. Maximum rates for 1000-hr exposures in refluxing initial and "average" condensates were 0.04 and 1.47 mils/mo, respectively, with little or no local attack.

---

\*Calcium sulfate "glasses" such as the one listed in Table 2.2 should have a greater thermal stability than the corresponding magnesium minerals. The thermograms in Figs. 2.4 and 2.5 do not apply directly to the corrosion data in Table 2.3. In laboratory glass-making experiments in stainless steel crucibles, catastrophic failure has often been observed, but never when the chemical equivalent ratio  $(\text{Na}+\text{Ca}+\text{Mg})/(\text{SO}_4^{--} + \text{PO}_3^- + \text{BO}_3^-) = 1.1$  and the temperature was kept below  $900^\circ\text{C}$ .

\*\*A nickel alloy with a composition similar to that of Ni-o-nel but with 0.003% maximum carbon.

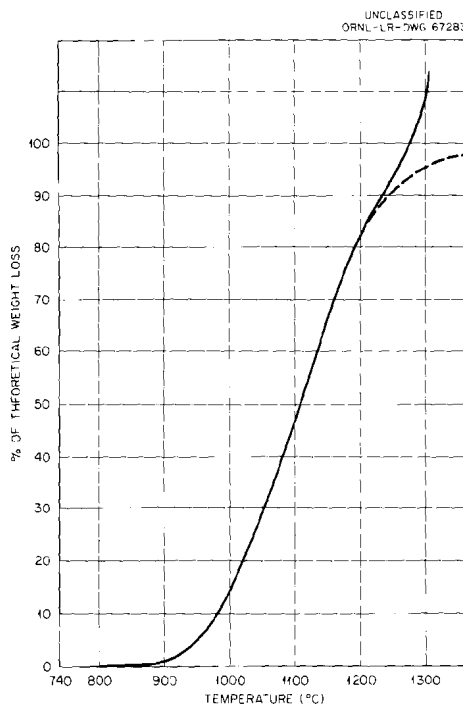


Fig. 2.4 Thermal decomposition of a magnesium borophosphate "glass" containing high-sulfate Purex waste. "Glass composition: 27.3%  $P_2O_5$ , 12.0%  $B_2O_3$ , 8.1%  $MgO$ , 15.9% added  $Na_2O$ , 36.7% waste oxides, softening point  $<825^\circ C$ . Initial weight 4.4010 g.

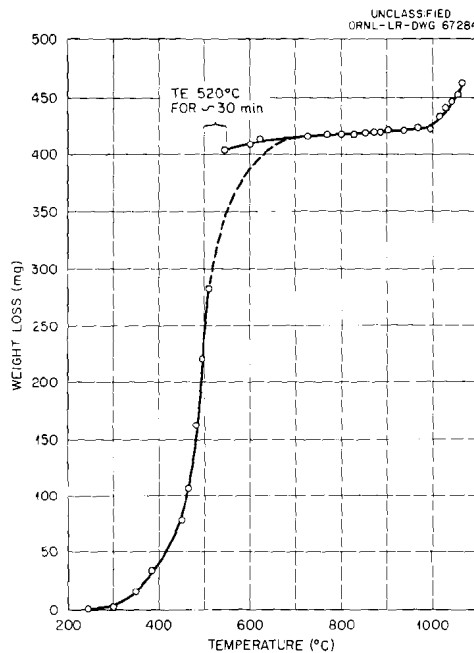


Fig. 2.5 Thermogram of the denitration and calcination of a mix for fixation of high-sulfate Purex waste in magnesium borophosphate "glass." "Glass" composition: 30.9%  $P_2O_5$ ; 3.4%  $B_2O_3$ ; 9.2%  $MgO_2$ ; 14.7% added  $Na_2O$ ; 41.6% waste oxides; softening point  $\sim 850^\circ C$ . Initial weight 1.8529 g.

LCNA and Hastelloy F showed grain boundary attack in the condensates expected from all solutions studied and in the vapor phase above boiling 6 M HNO<sub>3</sub> (Table 2.6b). The increase in corrosion rates with time in 6 M HNO<sub>3</sub>, from 0.62 to 2.35 for Hastelloy F and 0.80 to 1.89 for LCNA, respectively, for 168- and 672-hr exposures indicates increasingly aggressive localized attack, particularly under steady-state conditions, which would be encountered in a continuous process. The presence of peroxide had little if any effect on the corrosion of either alloy (Table 2.5c). It is not clear whether or not the presence of ruthenium exerted a real effect on the corrosion of Hastelloy F (Table 2.5b,c).

Type 347 stainless steel showed severe grain-boundary attack with overall rates as high as 3.58 mils/mo when exposed to refluxing initial Purex waste solution, although pot head flanges constructed of stainless steel have been used for a number of successive calcination experiments with simulated Purex and TBP-25 wastes with no signs of gross corrosion (Sect. 2.3.1). No metallographic examination has been made of any of these flanges, and the total exposure has not been logged for any of them.

### 2.3.2 TBP-25 Waste

Tests in simulated TBP-25 waste solution (Table 2.2) showed overall corrosion rates of 5.10 and 10.5 mils/mo for welded type 304L and 347 stainless steel, respectively, in 24 hr and 1.59 and 1.95 mils/mo in 68 hr (Table 2.3). These results indicate that aggressive corrosion ceases after volatilization of the free acid and the water. This was also found to be true for TBP-25 waste containing glass-making additives (Table 2.2); in two tests of 19 and 345 hr, overall corrosion rates were calculated to be 42.2 and 5.4 mils/mo, respectively (Table 2.3). The volume of condensate collected after 5-6 hr ( $T \approx 390^\circ\text{C}$ ) varied from 2 to 10% of the total (Table 2.4). No serious localized attack was apparent in either test. In both cases glassy melts formed which bonded tightly to the stainless steel, making separation of the specimen from the melt extremely difficult.

Semicontinuous fixation of 20-30 liters of TBP-25 waste as glass in a stainless steel pot with an unheated center well resulted in the steel in the well becoming magnetic below the final level of the glass. A few spots on the pot wall also became magnetic. Metallographic studies are being made to determine the nature of the magnetic transformation and its possible implications to container corrosion.

## 3.0 LOW-LEVEL WASTE TREATMENT

A scavenging-ion exchange process (8,9) is being developed for decontaminating the large volumes of slightly contaminated water produced in nuclear installations with ORNL low-activity-level waste as a medium for study. The process uses phenolic resins, as opposed to polystyrene resins, since the phenolic resins are much more selective for cesium in the presence of sodium; the Cs/Na separation factor is 160 for

Table 2.4 Distillation and Calcination of Simulated TBP-25 Waste Solution Plus Additives

Solution: 1.3 M  $H^+$ , 6.6 M  $NO_3^-$ , 1.72 M  $Al^{3+}$ ,  $\sim 0.003$  M  $Fe^{3+}$ ,  $\sim 0.02$  M  $Hg^{2+}$ ,  $\sim 0.0003$  M  $Ru^{3+}$ , 2.0 M  $NaH_2PO_2$ , 0.25 M  $PbO$

Expt. No.	Time after		Vol % of Starting Solution Collected in Condensate
	Startup (hr)	Avg Temp ( $^{\circ}C$ )	
1	1	140	28
	4	300	24
	5	390	24
	19	920	9.6
2	4	200	24
	5	280	36.8
	6	390	20
	345	910	1.6

phenolic groups and 1.5 for sulfonic groups. Other cations, e.g., strontium and rare earths, are also sorbed efficiently. Inorganic ion exchange media, such as vermiculite and clinoptilolite, are being studied as alternatives. The waste solution must be clarified prior to ion exchange since ion exchange media do not remove colloidal materials efficiently. Water clarification techniques are being developed for both the ion exchange processes and for the ORNL lime-soda process waste water treatment plant. Work is proceeding on both development and pilot plant programs.

### 3.1 Pilot Plant

Four demonstration runs were completed (Table 3.1), the volumes of ORNL process waste treated ranging from 55,000 to 90,000 gal, representing 1800-3100 resin bed volumes. Major contaminants, Sr-90 and Cs-137, were removed by factors  $>2000$  and  $>246$ , respectively (Table 3.1). The plant effluent contained  $<1.5\%$  of current  $MPC_w$  values for these isotopes for a 168-hr week. Run durations varied from 71 to 100 hr of continuous operation.

#### 3.1.1 Operation (R. E. Brooksbank)

In the second run, HR-3, the 10-in.-dia, 8-ft-high, Duolite CS-100 resin bed functioned satisfactorily for a total of 2000 bed volumes. After 1500 bed volumes had been treated, overall decontamination factors from Sr-90 and Cs-137 were 6143 and 788, respectively. Following a  $\gamma$ -radiation scan of the resin bed, and in the absence of a calcium breakthrough, operation was continued to 2086 bed volumes, when the decontamination factors from Sr-90 and Cs-137 were 2047 and 246, respectively, representing  $>99.5\%$  removal for both isotopes.

Table 2.5 Corrosion of Candidate Materials of Construction in Refluxing Initial High-Sulfate Purex Waste Solution

Solution composition: 5.6 M  $H^+$ , 6.1 M  $NO_3^-$ , 1.0 M  $SO_4^{2-}$ , 0.6 M  $Na^+$ , 0.1 M  $Al^{3+}$ , 0.5 M  $Fe^{3+}$ , 0.01 M  $Cr^{3+}$ , 0.01 M  $Na^+$ , 0.002 M  $RuCl_3$ . Duplicate specimens of all materials exposed.

Material	Specimen Position	Maximum Cumulative Corrosion Rate (mils/mo)									Remarks	
		24 hr	48 hr	72 hr	150-168 hr	294-312 hr	500-504 hr	672 hr	840 hr	1000 hr		
<b>a. Without Additives</b>												
Ti-45A	V	---	---	0.07	0.03	0.04	0.02	---	---	0.03	No local attack	
	I	---	---	0.07	0.03	0.04	0.03	---	---	0.03		
	S	---	---	0.04	g	g	0.02	---	---	0.04		
Hastelloy F	V	0.7	0.5	0.41	0.34	0.31	0.27	0.29	0.31	---	Grain-boundary, weld and edge corrosion	
	I	1.2	0.9	0.76	0.76	0.87	1.16	1.63	2.02	---		
	S	1.5	1.2	0.99	1.15	1.41	2.05	2.82	3.25	---		
LCNA	V	0.3	0.2	0.15	0.12	0.11	0.11	0.10	0.11	---	Grain boundary, weld, and edge corrosion	
	I	0.5	0.4	0.40	0.37	0.37	0.38	0.42	0.45	---		
	S	0.8	0.8	0.71	0.66	1.41	0.67	0.73	0.82	---		
Type 347 stainless steel	V	---	---	0.88	0.80	0.80	---	---	---	---	Severe grain-boundary attack	
	I	---	---	3.56	3.57	3.58	---	---	---	---		
	S	---	---	3.47	3.58	3.55	---	---	---	---		
<b>b. Effect of Ru and <math>Cl^-</math></b>												
Hastelloy F	V	Exposure Time (hr) and Solution						500				
		48		288								
		Ru <sup>c</sup>	No Ru <sup>c,b</sup>	Ru <sup>c</sup>	No Ru <sup>c,b</sup>	Ru <sup>c</sup>	No Ru <sup>b,c</sup>					
		0.53	0.21	1.1	0.2	1.4	0.2					
Hastelloy F	I	48		288		500						
		Ru <sup>c</sup>	No Ru <sup>c,b</sup>	Ru <sup>c</sup>	No Ru <sup>c,b</sup>	Ru <sup>c</sup>	No Ru <sup>b,c</sup>					
		1.52	1.63	1.6	0.9	2.5	1.0					
Hastelloy F	S	48		288		500						
		Ru <sup>c</sup>	No Ru <sup>c,b</sup>	Ru <sup>c</sup>	No Ru <sup>c,b</sup>	Ru <sup>c</sup>	No Ru <sup>b,c</sup>					
		2.74	2.74	2.2	1.3	2.8	1.9					
<b>c. Effect of <math>H_2O_2</math></b>												
Hastelloy F	V	24 hr <sup>d</sup>	48 hr <sup>d</sup>	72 hr <sup>e</sup>								
		0.72	0.54	---								
		1.23	1.06	---								
Hastelloy F	I	24 hr <sup>d</sup>	48 hr <sup>d</sup>	72 hr <sup>e</sup>								
		1.55	1.25	---								
		---	---	---								
LCNA	V	24 hr <sup>d</sup>	48 hr <sup>d</sup>	72 hr <sup>e</sup>								
		0.21	0.20	0.21								
		0.69	0.58	0.58								
LCNA	I	24 hr <sup>d</sup>	48 hr <sup>d</sup>	72 hr <sup>e</sup>								
		0.78	0.67	0.66								

<sup>a</sup> g indicates slight weight gain.

<sup>b</sup> Contained 0.006 M NaCl instead of 0.002 M  $RuCl_3$ .

<sup>c</sup> Only one specimen exposed.

<sup>d</sup> Solution spiked with 0.003 M  $H_2O_2$ .

<sup>e</sup> 0.003 M  $H_2O_2$  added continuously to refluxing solution.

Table 2.6 Corrosion of Candidate Materials of Construction in "Average" Condensate from High-Acid Purex Waste

Material	Specimen Position	Maximum Cumulative Corrosion Rate (mils/mo)										Remarks	
		24 hr	48 hr	72 hr	96 hr	120 hr	144 hr	288 hr	388 hr	520 hr	1000 hr		
a. Refluxing 6 M HNO <sub>3</sub> -0.05 M H <sub>2</sub> SO <sub>4</sub> , duplicate specimens exposed.													
Ti-45A	V	g	---	---	g	---	g	0.02	---	---	0.04	Little or no local attack	
	I		1.0	---	---	0.7	---	0.80	0.68	---	---		0.57
	S		2.1	---	---	1.9	---	2.1	1.41	---	---		1.47
Hastelloy F	V		0.65	0.52	0.53	0.48	0.49	0.44	---	1.27	2.85	Grain-boundary attack (vapor phase)	
	I		0.78	0.67	0.62	0.59	0.57	0.53	---	0.42	0.39		---
	S		1.02	0.83	0.73	0.66	0.63	0.58	---	0.45	0.41		---
LCNA	V		0.37	0.18	0.21	0.15	0.41	0.40	---	0.93	2.72	Grain-boundary attack (vapor phase)	
	I		0.35	0.23	0.19	0.16	0.17	0.15	---	0.15	0.18		---
	S		0.36	0.23	0.20	0.18	0.18	0.16	---	0.12	0.13		---
LCNA-0.2% Pt	V		1.9	---	---	4.3	---	3.6	---	---	---	Severe grain-boundary and pitting attack	
	I		3.5	---	---	5.9	---	7.0	---	---	---		
	S		4.4	---	---	6.5	---	7.2	---	---	---		
b. Refluxing 6 M HNO <sub>3</sub> , single specimen exposed.													
Hastelloy F	V		<u>168 hr</u>		<u>336 hr</u>		<u>504 hr</u>		<u>672 hr</u>			Grain boundary attack	
LCNA	V		0.62		1.19		2.01		2.35				
			0.80		0.79		1.36		1.89			Grain boundary attack	

Table 2.7 Corrosion of Candidate Materials of Construction in Final Refluxing Environments from Evaporation-Calcination of High-Sulfate Purex Waste

Duplicate specimens exposed.

Material	Specimen Position	Maximum Cumulative Corrosion Rate, mils/mo											Remarks
		24 hr	48 hr	72 hr	96 hr	120 hr	144 hr	331 hr	360 hr	499 hr	600 hr	1145 hr	
a. Refluxing 15 M HNO <sub>3</sub> -1 M H <sub>2</sub> SO <sub>4</sub> , estimated to approximate final condensate from an evaporation-calcination cycle.													
Ti-45A	V	0.77	---	0.76	---	---	0.72	---	g	---	0.28	0.33	Some local attack in heat-affected zone
	I	2.94	---	1.08	---	---	1.58	---	1.90	---	1.91	1.39	
	S	3.97	---	3.97	---	---	2.27	---	3.25	---	2.91	2.01	
Hastelloy F	V	6.25	6.39	7.45	8.20	8.86	9.83	9.81	---	11.24	---	---	Grain-boundary, edge and pitting attack
	I	4.40	3.72	3.39	3.49	3.56	3.79	4.61	---	4.73	---	---	
	S	4.83	4.09	3.87	3.90	4.03	4.23	5.47	---	5.96	---	---	
LCNA	V	0.47	0.54	0.63	0.44	0.69	0.65	0.60	---	9.88	---	---	Grain-boundary attack
	I	1.60	1.27	1.15	1.07	1.01	0.98	0.89	---	0.91	---	---	
	S	1.85	1.36	1.23	1.12	1.07	1.02	0.88	---	1.03	---	---	
b. Final High-Sulfate Purex Waste Solution: 0.3 M H <sup>+</sup> , 1.3-1.8 M NO <sub>3</sub> <sup>-</sup> , 2.0-3.0 M SO <sub>4</sub> , 1.2-1.8 M Na <sup>+</sup> , 0.2-0.3 M Al <sup>3+</sup> , 1.0-1.5 M Fe <sup>3+</sup> , 0.02-0.03 M Cr <sup>3+</sup> , 0.02-0.03 M Na <sup>2+</sup> , 0.004-0.006 M Ru <sup>3+</sup> .													
Hastelloy F	V	24 hr	48 hr	72 hr									
		g	0.12	0.10									
	I	g	0.11	0.11									
LCNA	V	0.10	0.08	0.08									
	I	0.41	0.14	0.09									
	S	0.32	0.06	0.11									

Table 3.1 Removal of Activity from ORNL Process Waste

Run No.	Bed Vol	Gross $\beta$		Gross $\gamma$		Sr-90		Sr-89		Co-60		TRE		Cs-137	
		D.F.	% Re-moved	D.F.	% Re-moved	D.F.	% Re-moved	D.F.	% Re-moved	D.F.	% Re-moved	D.F.	% Re-moved	D.F.	% Re-moved
HR-2 <sup>a</sup>	1600	30	96.7	44	97.7	2956	>99.9	---	---	16	93.9	4	71.6	288	99.7
HR-3	2100	46	97.8	25	96.1	2047	>99.9	---	---	11	91.3	28	96.5	246	99.6
HR-4	2000	42	97.6	10	89.9	4982	>99.9	3117	>99.9	6	82.8	22	95.6	429	99.8
HR-5	1800	37	97.3	16	93.8	5588	>99.9	---	---	4	74.3	31	96.8	2520	>99.9

<sup>a</sup>Included for comparison; analytical data for run HR-6 not yet complete.

In runs HR-4 and HR-5 made with an 18-in.-dia, 18-in.-high bed, no adverse effects were noted. Decontamination factors from Sr-90 and Cs-137 were higher for both isotopes (Sr = 4982 - 5588, Cs = 429 - 2520) than in run HR-3; however, the feed activity was higher and the detection of the isotopes in plant effluent solutions was at or below the limits of analytical detection. The major contaminant in plant effluent solution, although still below MPC<sub>w</sub> requirements, was Co-60.

Analytical data are not yet complete for run HR-6, made with the 10-in.-dia resin bed, but a Sr-90 breakthrough equal to the MPC<sub>w</sub> (2.22 d/m.ml) was detected between 2500 and 2700 bed volumes, and a hardness breakthrough after 2780 bed volumes.

Ion Exchange. The use of the "split" elution technique, which decreases the volume of spent solution leaving the process, was successfully demonstrated. In this procedure, 5 vol of 0.5 M HNO<sub>3</sub> from the tail-end of the previous elution is used as the initial eluant. The second 5 vol, with a very low fission product concentration, is held in storage for subsequent elution cycles. Typical elution curves are shown in Fig. 3.1.

The use of a movable  $\gamma$  radiation probe through the length of the bed proved to be an effective tool for anticipating resin column breakthrough. Throughout each run, the location of the maximum radiation band was noted as a function of resin bed volumes passed through the column (Fig. 3.2). A double peak in the bed at 1757 bed vol is probably due to the increased delivery of calcium to the resin columns. Shortly after 1500 bed vol, the sand filter effluent increased in hardness from 8 to 16 ppm (as CaCO<sub>3</sub>). The formation of the second peak was established after the change was made to anthracite filtration.

Data Tabulation. A simple Fortran program was written to speed the tabulation and calculation of process data.

### 3.1.2 Equipment Performance (W. R. Whitson, J. O. Blomeke)

Continuous performance of the pilot plant equipment under designed flowsheet conditions was satisfactorily demonstrated in runs HR-3 through 6 except for erratic performance of the vacuum sludge filter and a minor difficulty with the clarifier.

The Oliver rotary-drum vacuum filter did not remove the sludge from the clarifier efficiently. The sludge penetrated the precoated surface of the drum to a depth of  $\sim 1/16$  in., forming an impervious layer through which it was impossible to maintain an adequate solids drawoff rate. This and other malfunctioning variables required constant attention of the operators. Modifications were made to the Eimco plate-and-frame pressure filter so that the use of a pressure type filter would meet the approval of the Radiation Control Officer. These consisted in simplifying cake removal by enclosing the filtered sludge cake in a canvas filter bag completely contained in the cavity formed by the frame and two end plates. The necessity for

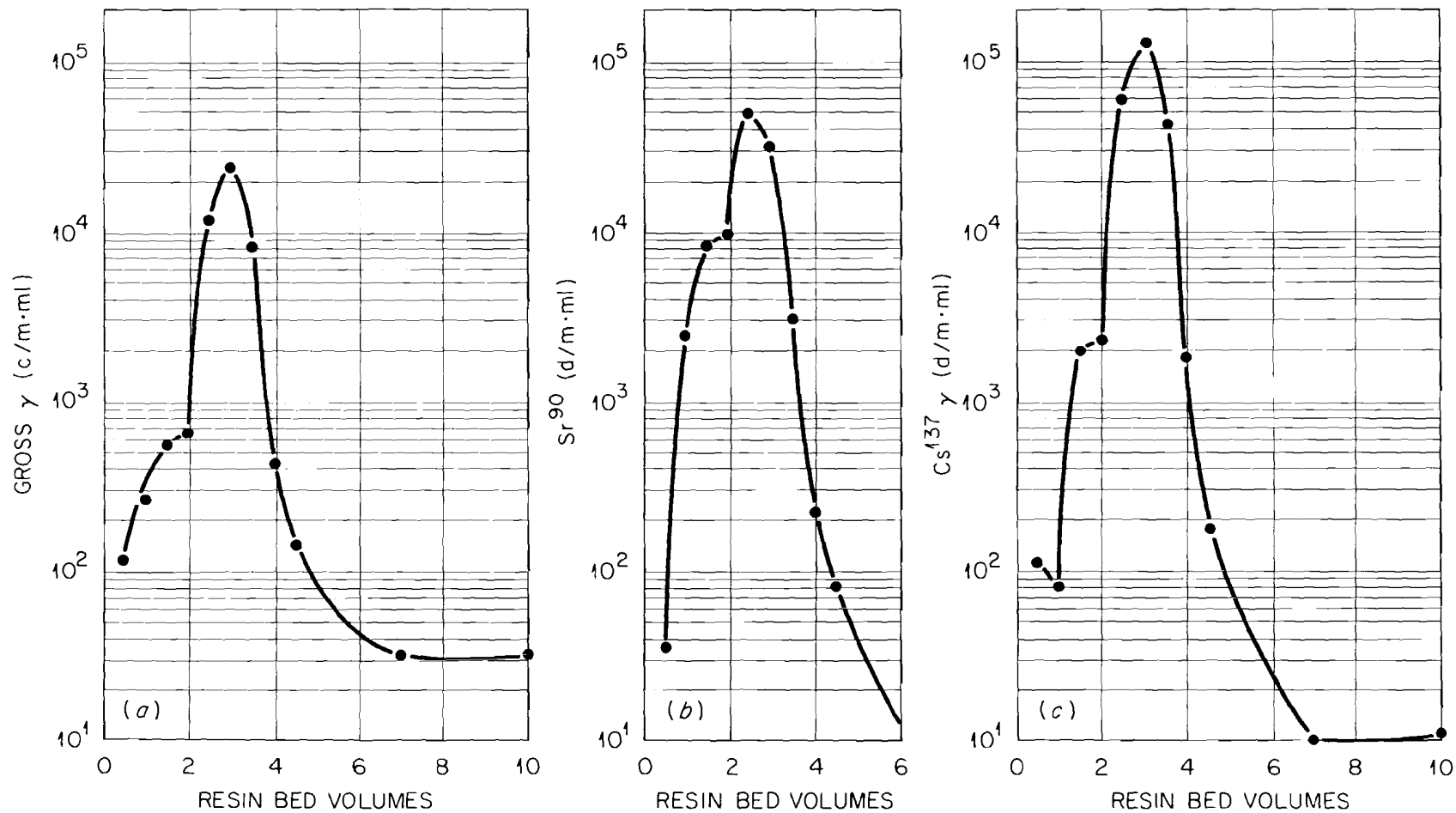


Fig. 3.1 Elution of (a) gross  $\gamma$ , (b) Sr-90, and (c) Cs-137 from Duolite Cs-100 resin with 0.5 M HNO<sub>3</sub> (run HS-3).

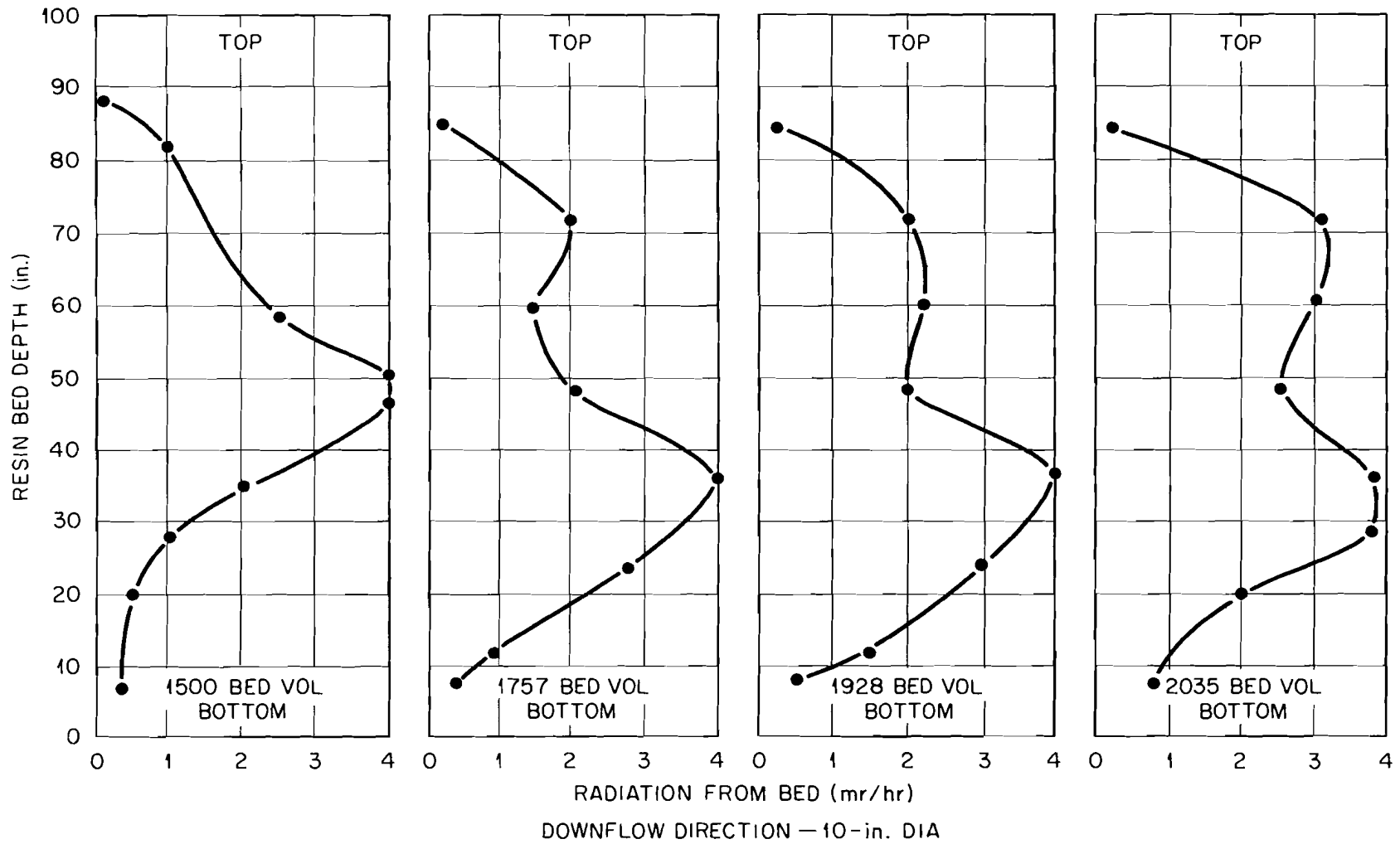


Fig. 3.2 Resin radiation profile during elution (run HR-3). Downflow elution; 10-in.-dia column.

putting elaborate containment around this unit has been eliminated since the filter cake is not openly exposed to the atmosphere, and, being compact and neatly packaged in the bag, it is easily handled by operating personnel and conveniently disposed of in sealed drums.

Supersaturation of the effluent overflowing the clarifier caused excessive scale buildup on the walls of some of the equipment and piping. This scale coated the piping, pump, and control valve located between the clarifier and polishing filters. Most of these particles are removed by the polishing filters prior to entering the ion exchange columns, but, due to excessive amounts of the  $\text{CaCO}_3$  particles in the effluent, the filtering time of each filter shortened, necessitating frequent back-washing of the filter beds. Facilities for recycling a portion of the sludge to the flocculator are being added to the system to alleviate the supersaturation problem by providing additional nuclei to aid precipitation.

### 3.2 Laboratory Studies (R. R. Holcomb, W. E. Clark)

Pilot Plant Effluent. A strong base anion exchange column, 7/8 in. i.d. by 6 in. high, sorbed cobalt and ruthenium from 1500 bed volumes of treated pilot plant effluent on the top 2 in. as shown by a gamma energy scan of the resin.

Vermiculite Evaluation. In preliminary laboratory-scale studies, difficulties were encountered in the use of vermiculite as an ion-exchange medium for second stage removal of fission products from low activity wastes, but evaluation studies are continuing. Five small columns, 7/8 in. i.d. by 6 in. high, containing BO-4 grade vermiculite were installed on the filter effluent stream of the pilot plant to operate with ~8 ft of head at liquid flow rates of 1, 5, 15, 30 and 40 ml/min. The faster rates decreased to 4-5 ml/min during the first 24 hr operation, but normal rates were restored by loading the columns with vermiculite that had been thoroughly back-washed to remove fines, 25-50% of the total. The columns then became saturated with solids from an unnoticed pilot plant polishing filter breakthrough. The contaminated vermiculite was replaced and a 5- $\mu$  cellulose filter was placed in the system to protect the exchanger. The solids from the filter breakthrough caused only a slight pressure drop increase across the relatively large mesh organic ion-exchange resin in the pilot plant columns and would not continue to increase since they are removed by the acid treatment every 3 days. However, to be competitive with organic resins, vermiculite must remain on stream for up to 30 days. This lengthy operation with the very small mesh vermiculite would undoubtedly result in complete stoppage as occurred in the small test columns.

Control Analysis. While difficulty was previously encountered in pilot plant water analysis with Nalco reagents when using the manufacturer's prescribed procedures, these reagents were satisfactory for the high pH streams when little or no buffer was used. Accuracy was 1 ppm in neutral-high hardness or high pH-low hardness waters, particularly when a blank of distilled water was used for end-point comparison. Some difficulty is still being encountered with neutral-low hardness (1-5 ppm) water.

Head-End Treatment. A series of standard jar tests has been initiated with ORNL tap water as a feed solution in the hope of improving the pretreatment portion of the low level waste treatment flowsheet. The tap water had the following average macrochemical composition: total hardness, 109 ppm as  $\text{CaCO}_3$ ; calcium hardness, 77 ppm as  $\text{CaCO}_3$ ; magnesium hardness, 32 ppm as  $\text{CaCO}_3$ ; and total alkalinity, 101 ppm as  $\text{CaCO}_3$ . In the first set of tests, cold lime (only) treatments varying from 31 to 190 ppm  $\text{Ca}(\text{OH})_2$  resulted in varying residual equilibrium hardnesses starting at 74 ppm, decreasing to a minimum of 53 ppm, and then increasing to 127 ppm (Fig. 3.3).

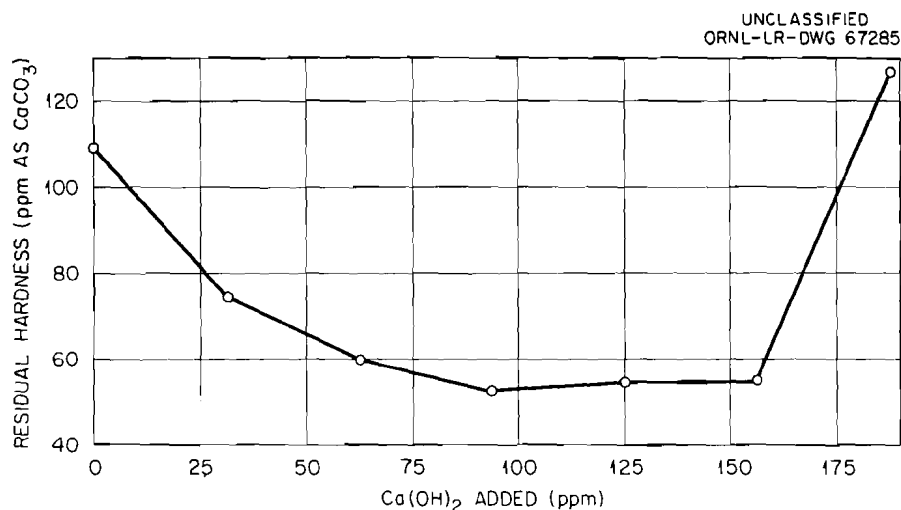


Fig. 3.3 Removal of residual hardness from tap water with calcium hydroxide.

In a second set of tests in which stoichiometric cold lime and varying amounts of a cationic polyelectrolyte coagulant were added, a more heterogeneous floc was formed and a final more turbid water resulted than when lime alone was used. A third set of tests was run under standard flowsheet conditions, caustic-copperas treatment, with varying amounts of  $\text{HCO}_3^-$  and  $\text{CO}_3^{=}$  to determine if a carbonate deficiency existed. Carbonate additions from zero to 500 ppm had little or no noticeable effect on the resulting water quality whether added before, with, or after the other chemicals.

#### 4.0 ENGINEERING, ECONOMIC AND HAZARDS EVALUATION

R. L. Bradshaw, J. J. Perona, and J. T. Roberts

A comprehensive study has been undertaken to evaluate the economics and hazards associated with alternative methods for ultimate disposal of highly radioactive liquid and solid wastes. All steps between fuel processing and ultimate storage will be considered, and the study should define an optimum combination of operations for each disposal method and indicate the most promising methods for experimental study.

Space requirements to dissipate the fission product heat in the waste from a 56,000 Mw(th) nuclear power economy were calculated for cylinders of calcined waste buried in a vertical position in the floors of rooms in salt media. Acres per year of mined space required was calculated for Purex and Thorex wastes in acidic and re-acidified forms in 6-, 12- and 24-in.-dia vessels buried at ages of 0.33 to 30 years. Calculations were made also for an acidic Thorex glass in 6-in.-dia vessels.

The maximum allowable temperatures in the salt and in the calcined wastes were chosen to be 400 and 1650°F, the same as they were in the calculation of space requirements for the storage of calcined wastes above the floor in salt rooms (2). The cylindrical vessels, 10 ft long, were assumed to be arranged in vertical holes 33% larger in diameter than the vessel diameter (e.g. 8-in.-dia holes for 6-in.-dia vessels) and 15 ft deep, with the top 5 ft occupied by salt or concrete plugs for shielding purposes. Temperature profiles in the salt were calculated from the equation for a finite decaying line source in an infinitely long perfectly insulated cylinder of salt (10). Temperature drops from the waste cylinder axis to the surface of the hole in the salt were calculated by the same basic equations as those used for storage above the floor except that the convective heat transfer coefficients were calculated from the following equation for vertically enclosed air spaces (11):

$$\frac{hx}{k} = \frac{C}{(L/x)^{1/9}} [N_{Gr} \cdot N_{Pr}]^n$$

where  $h$  = convective heat transfer coefficient based on the temperature difference between the two surfaces

$x$  = distance between surfaces

$k$  = thermal conductivity of fluid

$L$  = height of enclosed space

$N_{Gr}$  = Grashof number

$N_{Pr}$  = Prandtl number

$n = 1/4$  and  $C = 0.20$  for  $2 \times 10^4 < N_{Gr} < 2.1 \times 10^5$

$n = 1/3$  and  $C = 0.071$  for  $2.1 \times 10^5 < N_{Gr} < 1.1 \times 10^7$

The minimum spacing for acidic Purex in 6- and 12-in.-dia cylinders ranged from 20 and 36 ft at minimum burial age to 10.5 ft and 23 ft at 30 years, respectively. Acidic Purex cannot be stored in 24-in.-dia cylinders in this manner at ages below 30 years. The minimum spacing for reacidified Thorex in 6- and 24-in.-dia cylinders ranged from 6 and 20 ft at minimum burial age to 10 ft at 30 years.

The net area requirements for Purex waste calculated from cylinder production rate and cylinder spacing range from 20 acres/year at 0.65 year to about 2 acres/year at 30 years burial age. Corresponding results for Thorex wastes were 10 and 0.7

acres/year (Figs. 4.1-4.3). The primary effects of the form of the waste (acidified, reacidified, glass) and vessel diameter are to limit the minimum burial age, although area requirements may be affected by factors of 2-3 by waste form and vessel size near the minimum burial ages.

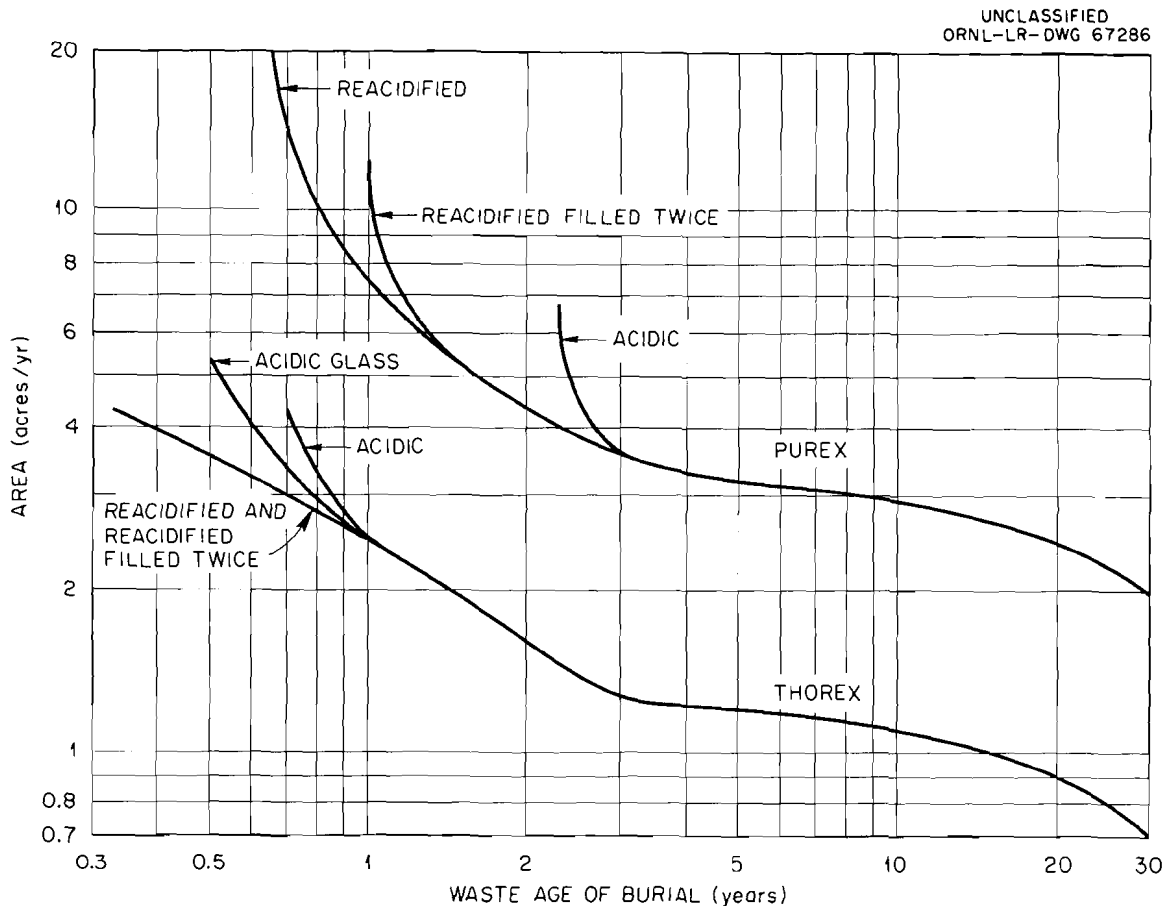


Fig. 4.1 Net area requirements for storage of 6-in.-dia vessels of Purex and Thorex waste in floor of salt mine.

## 5.0 DISPOSAL IN DEEP WELLS

### 5.1 Disposal by Hydraulic Fracturing (W. de Laguna and T. Tamura)

#### 5.1.1 Second Fracturing Experiment (W. de Laguna)

The purpose of the second fracturing experiment was to determine if conformable fractures would be formed in the Conasauga shale under conditions approximating those of an actual disposal operation and the pressures that would be required. Two injections were made into the same well, one at a depth of 1000 ft and the other at 700 ft, and for each injection 100,000 gal of water containing sufficient cement and other

UNCLASSIFIED  
ORNL-LR-DWG 67287

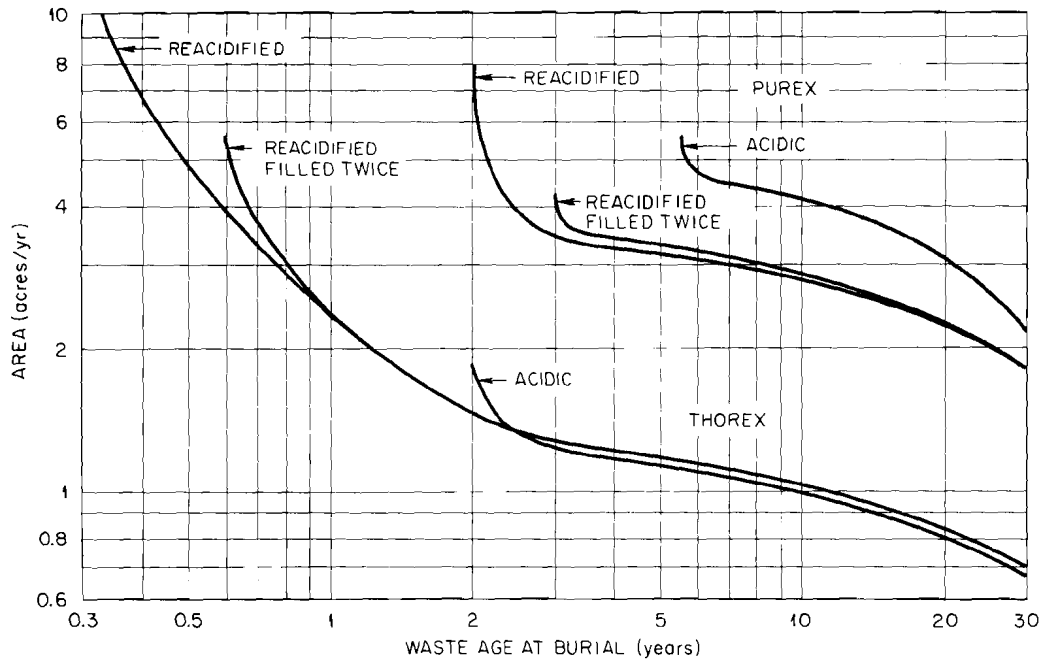


Fig. 4.2 Net area requirements for storage of 12-in.-dia vessels of Thorex and Purex waste in floor of salt mine.

UNCLASSIFIED  
ORNL-LR-DWG 67288

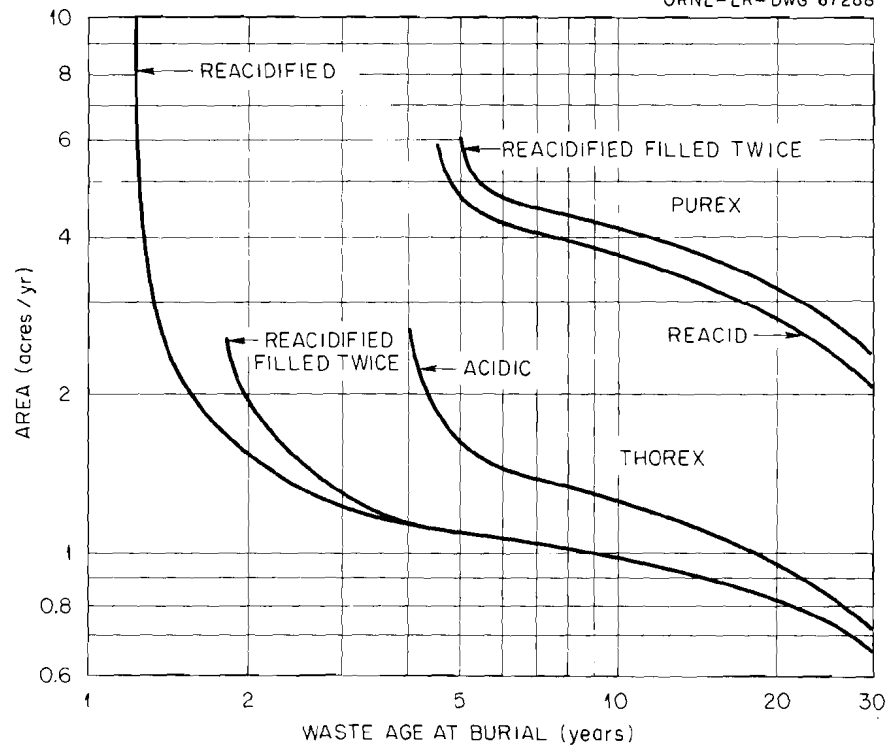


Fig. 4.3 Net area requirements for storage of 24-in.-dia vessels in floor of salt mine.

additives to give a crushing strength of 500 psi after 28 days was used. A subcontract was awarded to the Halliburton Company (Duncan, Oklahoma) for cementing in the casing and injecting the two batches.

Site Preparation. A site was selected in Melton Valley, about 6000 ft east of the site of the first experiment and about 1500 ft south of the stratigraphic position of the top of the first fracturing well. It was estimated that the horizon fractured in the first experiment would be encountered at a depth of roughly 700 ft and that the top of the Rome sandstone would be at about 1000 ft. The well-bedded red noncalcareous shale that occupies the interval between the three limestone beds and the Rome was believed to be best suited for the experiment. Water was provided at the site by a 4-in. potable-water pipeline running from the Homogeneous Reactor Experiment area to the Tower Shielding Facility on Melton Hill. Electric current for lights and the Milton-Roy pump was available from a power line, and an old dirt road was regraded and rocked to provide access for heavy equipment.

Two wells, 30 ft apart on strike, were drilled to a depth of 1050 ft. The first was 8 in. dia with a heavy-duty standard churn drill normally used for drilling water wells. This diameter was drilled to provide sufficient annular space between the rock wall of the well and a 4.5-in.-o.d. casing to ensure a good cement job on the casing. A 4-in.-i.d. casing was required so that it could be slotted with a sand jet, a standard procedure in oil fields. The well was drilled without incident, although progress was slow between 950 ft and the bottom, in which interval the very hard sandstone forms the upper part of the Rome formation.

To select the exact horizons for fracturing, a second well, a 3-in.-dia (NX-size) core hole, cored all the way, was drilled 30 ft west of the 8-in. injection well. When it was completed, both wells were logged by the U. S. Geological Survey with a "Widco" gamma-ray logger. A string of pipe was placed in the hole, consisting (measuring up from the bottom) of 158 ft of perforated 1.5-in.-dia pipe, a packer, and 892 ft of 3/4-in. pipe to the surface. The core hole was then backfilled with cement by pumping it down a 1/2-in. pipe run down into the annular space between the 3/4-in. pipe and the side of the hole as far as the packer. This 1/2-in. pipe was removed, section by section, as the annular space was filled. The completed operation left ~158 ft of open hole at the bottom of the 3-in. well connected to the surface by 3/4-in. pipe firmly cemented into place.

A network of 33 bench marks was set on six lines radiating out from the injection well. The relative elevations of the bench marks were determined by J. H. Langhofer and M. J. Mannello of the Topographic Division of the U. S. Geological Survey, using special high-precision equipment. The measurements were reported to the nearest ten-thousandth of a foot (hundredth of an inch). The bench marks were re-surveyed after the first injection and again after the second injection to observe the pattern of surface uplift. Several additional bench marks were set to provide support for special hydraulic tilt meters used by F. Riley of the USGS to measure crustal movement during the injections. This work is reported elsewhere (12).

The 4-in. casing was lowered into the 8-in. hole and cemented into place on Aug. 2, 1960 (Fig. 5.1). The isotope feed tank and Milton-Roy pump were arranged as in the first experiment.

Injection into First or Lower Fracture. The equipment used for the first injection was: (1) one 58 A pumping truck with two pumps for mixing and injecting the cement grout, (2) one single A-C pump unit for mixing bentonite and water, (3) one A-C pump unit for stand-by, (4) one Moyno pump unit for stand-by, (5) 1000 ft of 2-in. pipe for cutting slot, (6) one 800-ft<sup>3</sup> bulk storage bin for cement, (7) one 1400-ft<sup>3</sup> bulk storage bin for cement, (8) various connections and hose, and (9) a flow meter for measuring water and proportioning bentonite. The bulk dry cement was delivered to the site by the Concrete Supply Company (Knoxville, Tennessee). The bins were filled the day before, and additional cement was delivered during the injection operation in 20-ton bulk cement transport trucks.

On September 2, the casing was slotted at a depth of 934 ft with a 3/16-in. 4-way Hydra-jet gun, using 4000 lb of 20- to 40-mesh sand in 7000 gal of water slightly thickened with bentonite. The cut was accomplished by pumping for 7 min at 2300 psi and 38 min at 3500 psi. The pipe supporting the gun was rotated and moved up and down slightly due to pulsing from the pumps; therefore the slot cut through the casing and out into the shale was about 1 in. wide.

At 9:00 a.m. on September 3, the fracture was initiated with water. The well "broke down," that is, the rock fractured at 1500 psi surface pressure. After break-down the surface pressure fell to 1350 psi at 140 gpm pumping rate, and then increased to a maximum of 1640 psi. After 6 min, by which time 850-900 gal of water had been pumped, the fracture broke into the open-hole section of the nearby core hole, where the pressure suddenly rose to 800 psi. Pumping was continued for about 15 min, during which time 1200 gal of water was injected. When the injection rate was slowed, pressure in the core hole fell to 700 psi; when pumping stopped, pressure in the core hole fell to 600 psi, and then slowly dropped to 510 psi after 20 min (9:35), and to 360 psi after an hour and a half (10:50).

C. D. Wicker (Operations Division) and E. L. Sharp (Applied Health Physics) transferred 25 curies of Cs-137 to the feed tank (Fig. 5.2). Injection of the grout mixture and tracer were begun at 11:00 a.m. at initial rates of 125 gpm and 1.7 gph, respectively. The initial injection pressure for the grout was 2300 psi, but this dropped erratically over a period of a few minutes to 1700-1750 psi. During the first half hour of pumping, there were rapid pressure surges from a base pressure of 1700-1750 psi up to 2000-2200 psi.

After 9 min of grout injection, grout broke into the open-hole section of the core hole, and the pressure on this well suddenly rose to 1400 psi. Pressure readings on this gage also showed surges during the next 20 min or so, and then a very slow rise to 1500 psi at 1:00 p.m., and to 1700 psi at 2:00 p.m. It then dropped slowly to

UNCLASSIFIED  
PHOTO 50974



Fig. 5.1 Site preparation for second fracturing experiment. The injection well in the background has been drilled, and the Halliburton crew is engaged in cementing in the casing. The pre-injection core hole to the left is nearly completed.



Fig. 5.2 Adding the Cs-137 concentrate to water in the shielded drum preparatory to the first injection of the second experiment. Left to right: C. D. Wicker, E. L. Sharp, and W. H. Longaker, project engineer.

1500 psi at 3:20 p.m. and varied between 1500 psi and 1650 psi until the injection was stopped at 10:00 p.m. The average pumping rate for grout injection was 138 gpm and the maximum rate, 156 gpm.

Pressure in the injection well remained at an average value of 1750 psi from about 9:30 a.m., by which time the more rapid pressure surges had died out, until the injection stopped, although it did increase briefly to 2000 psi at 9:25 p.m. The continuous chart recording made by the Halliburton Company indicated a slow, regular increase in pressure on the injection well from 1700 psi to 1750 psi at 9:30 a.m., by which time the surges had died out, to 1900 psi at 10:00 p.m. Between 10:00 p.m. and 10:10 p.m. a thick cement grout, without tracer or bentonite, was pumped into the well to seal the fracture and "chased" with enough water to force the upper surface of the cement down to a depth of 700 ft.

Total injection time, 11 hr, was longer than anticipated, because the pressures required were higher than expected. It was necessary, therefore, to reduce the pumping rate of the isotope tracer from 1.7 to 1.2 gph from about 12:00 noon until 8:20 p.m. Virtually all the tracer was injected.

A total of 91,567 gal of grout was injected, preceded by 1200 gal of water. The grout mixture contained 567 gal (12,500 lb) of bentonite and 16,000 gal (4440 sacks or 420,000 lb) of Portland cement. The density of the grout was 12.5 lb/gal, and its estimated viscosity was 15-20 poises.

During the greater part of the injection, the pressure gage on the core hole read 1500 psi. A 936-ft column of water would add 400 psi, to give a total pressure in the fracture of 1900 psi. At the same time, the well-head pressure on the injection well was about 1750 psi. A column of grout, 936 ft deep and weighing 12.5 lb/gal, would add 600 psi, for a total pressure of 2350 psi in the fracture. The difference between 2350 and 1900 psi presumably represents friction loss. The pressure required to pump into the fracture was substantially higher than the rule-of-thumb value of 1 psi per foot of depth.

Injection into Second or Upper Fracture. On September 9 the injection well was again slotted with the sand jet at a depth of 694 ft. Nine thousand pounds of 20- to 40-mesh sand was used, and the pumping required 30 min.

Water was then pumped into the well and the formation fractured at 1800 psi. After breakdown the pumping rate was increased to 275 gpm at 2500 psi. After 20 min of pumping at approximately this rate, the pressure had dropped to 2000 psi. When pumping stopped, the static pressure was 1500 psi. A total of 16,000 gal of water was injected at this time and released from the well at the end of the day.

Prior to this pumping, pressure on the core hole was 600 psi. Seven minutes after the fracture was initiated, pressure in the core hole was 700 psi; 9 min after, it was 675 psi; and after 17 min, it rose rapidly to 850 psi. After pumping was

stopped, pressure in both wells dropped slowly and in 1.5 hr had reached 800 psi in the core hole and 1000 psi in the injection well.

On the morning of September 10, 4000 gal of water was pumped into the injection well at a rate of 250 gpm and a pressure of 1800 psi to 2000 psi. Pressure in the core hole had dropped overnight to 625 psi, and during this initial pumping rose to 650 psi.

Wicker and Sharp transferred 25 curies of Cs-137 and about 2 curies of Co-60 to the feed tank. Cobalt was added to make it possible to distinguish between grout pumped into the first and second fractures. The main grout injection was started at a rate of 230 gpm and a pressure of 2200 psi (Fig. 5.3). Because small lumps of very hard rock in the cement broke the pump valve or valve springs several times, the pumping rate varied irregularly, and the pumps were shut down twice for periods of up to 20 min. The injection pressures varied accordingly, but averaged 2000 psi at 200 gpm and 2300 psi at 300 gpm. Pumping was stopped at 6:30 p.m. after 11 hr elapsed time and 10 1/2 hr of actual pumping. The total volume of grout pumped was 132,770 gal; so the average pumping rate was 210 gpm. The volumes pumped on September 10 were: water prior to grout, 4000 gal; water in grout, 102,000 gal; bentonite, 770 gal (17,000 lb); cement, 30,000 gal (8333 sacks, or 800,000 lb); density, 12.5 to 12.6 lb/gal.

At the close of pumping, enough water was pumped down the well to flush the last of the grout out into the fracture and leave the inside of the well casing full of water. The well was then shut in with valves at the well head.

Pressure Changes in and Flow from the Fractures Subsequent to Injection. On the day after the first injection (September 4), pressure on the injection well was 340 psi (the concrete plug was still setting) and on the core hole, 900 psi. On September 7, pressure on the injection well was 10 psi (the concrete plug had set) and on the core hole, 700 psi. One gallon of water was bled from the core hole and the valve was shut. The pressure immediately rose to 700 psi, showing that this well was connected to the fracture and not plugged with grout. On September 8, pressure on the core hole was 650 psi, and it fell gradually so that on the tenth, just prior to the second injection, the pressure was 600 psi.

After the second injection on September 10, pressures in the two wells were:



Fig. 5.3 Injection of second (upper) seam of second experiment. T-10 unit pumping grout is in center foreground. Behind pumper is lead block shield of tracer feed drum, and left of the drum is the injection well, fed by twin high-pressure lines from pumper. Left background is 20-ton bulk cement carrier, and behind the shielded isotope drum is the mobile change house.

Date	Well Injection, upper fracture (psi)	Core Hole, lower fracture (psi)
Sept. 11	580	575
12	475	560
13	425	560
14	380	545
16	340	525
21	290	475
22	290	475
23	275	465
26	250	450
27	245	440
28	240	435
29	235	425
Oct. 3	225	420
4	225	410

After these readings had been made, the injection well valve was opened. The well flow at first was 0.33 gpm, which decreased to 0.25 gpm after 10 min. On October 5 the flow was back up to 0.32 gpm, after which it slowly declined as follows: October 6, 0.285 gpm; October 7, 0.238 gpm; October 11, 0.160 gpm; November 1, 0.045 gpm; December 21, 0.0053 gpm.

By Jan. 1, 1961, the flow was a drop every few minutes, and a total of 6000 gal of water had been released from the well. By March 1 the rate was 0.33 gal/day. By April 1, 1961, the flow had ceased, and by May 1, the water level in the well had fallen 18 in. below the outlet. On September 11, the water level in the well was 16.35 ft below land surface, and on November 21, 16.20 ft below land surface. This is well below the water table.

The core-hole pressure was 385 psi on October 13, when it was opened to flow. From then to December 21, 2100 gal flowed, at first at a maximum rate of 0.05 gpm, and at the end at a rate of 0.005 gpm. The well was then again shut in, and the pressure rose to 200 psi on or before January 5, when it was next observed. Subsequent readings were: April 15, 160 psi; August 18, 115 psi; September 11, 110 psi; and November 1, 100 psi. On November 1, the well was again opened up and flowed at a rate of a drop every few seconds.

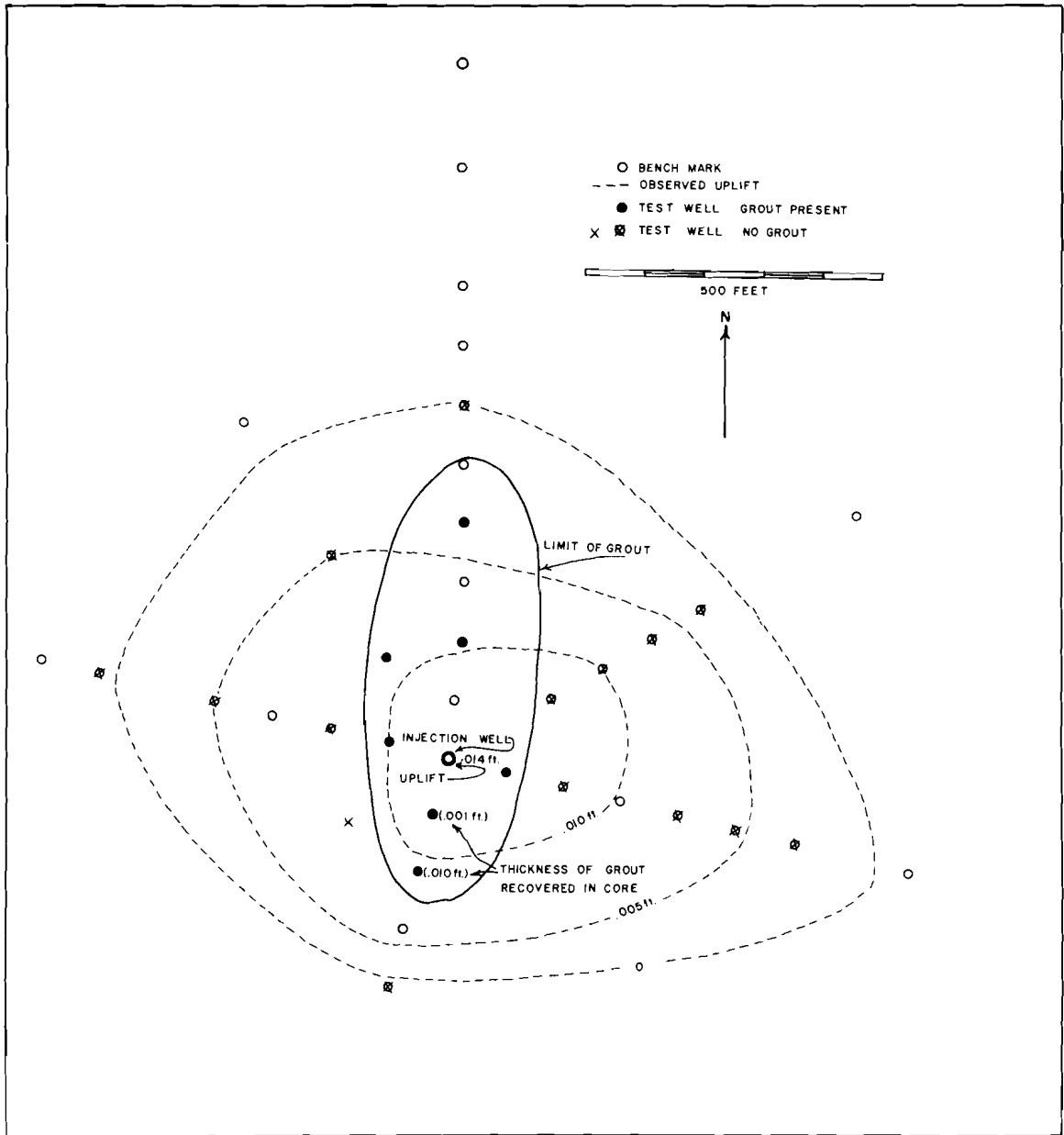
The flow from both wells consisted of water and gas in roughly equal proportions. The gas was 94% nitrogen, 5% methane, and 1% oxygen. The methane came from the shale.

Test Drilling. The five rock units identified in cross sections of the area of the second fracturing experiment are: (1) hard gray sandstone, (2) red shale, (3) gray calcareous shale, (4) three beds of limestone just above the contact between the gray and red shales, and (5) a single bed of limestone in the gray shale 200 ft above this contact. These five units, and the contacts between them, sufficiently describe the general structure of the area for the purposes of the experiment. Uncertainties as to the structure derive not from a lack of more key horizons or from uncertainties as to the position of these units in the test wells, but from the limited number of wells that can be drilled to these depths. Twenty-two test wells were drilled after the injections of the two fractures, eight by the Army Corps of Engineers and fourteen by ORNL.

Extent of the Lower Grout Sheet (Fig. 5.4). The lower grout sheet was found in the following test wells: 200 N, 400 N, 200 NW, 100 E, 100 S, 200 S, 100 W, but not in wells drilled farther out. These data suggest that the grout sheet, oriented north and south, is about 800 ft long by 300 ft wide, or approximately 240,000 ft<sup>2</sup>. Only two cores of the lower grout sheet were recovered, from wells 100 S and 200 S. The grout in 100 S was only paper-thin, but the gamma-ray logging suggests that the thickness of 0.01 ft, measured in the core from 200 S, is more nearly representative. This thickness also corresponds with the observed uplift of the land surface over the general area of the grout sheet, indicating an effective volume for the lower grout sheet of approximately 2400 ft<sup>3</sup>. The lower grout sheet contained 420,000 lb of Portland cement, which would take up an estimated 20% of its dry weight of water to give a total weight of about 500,000 lb. The grout has a measured air-dry density of 106 lb/ft<sup>3</sup>, so that there should be 4750 ft<sup>3</sup> of grout in place. The grout sheet must be both more extensive and thicker than these data suggest, but the material balance is poor.

The cross sections (Fig. 5.5 and 5.6) indicate that the lower grout sheet was displaced upward at some point near the injection well and then spread out laterally, following this new horizon. Both cross sections show that the injection well was drilled into a structural low, either a graben or a syncline, and that in moving out laterally from the injection well, the fracture came up against the hard Rome sandstone in a distance of 50 ft or so. The sandstone, virtually impenetrable to the fracture, must have deflected the grout upward about 80 ft. At this new level it spread out again in a north-south direction, suggesting that the confining structure extends in a general north-south direction. If this is indeed what happened, the experiment was a far more severe test of the possibility of developing conformable fractures in the shale than was intended.

The cross sections and the interpretations, based on these sections, rest on the assumption that the test wells are essentially vertical. This may not be the case, but a considerable departure from vertical of both the core hole and the injection well would be required to explain the observed data. Arrangements have been made to survey the bore holes with a photclinometer. A new test well is now being drilled midway between the core hole and the injection well, and data from it will probably resolve some of the present uncertainties.



5.4 Lower grout sheet of second fracturing experiment and observed uplift.

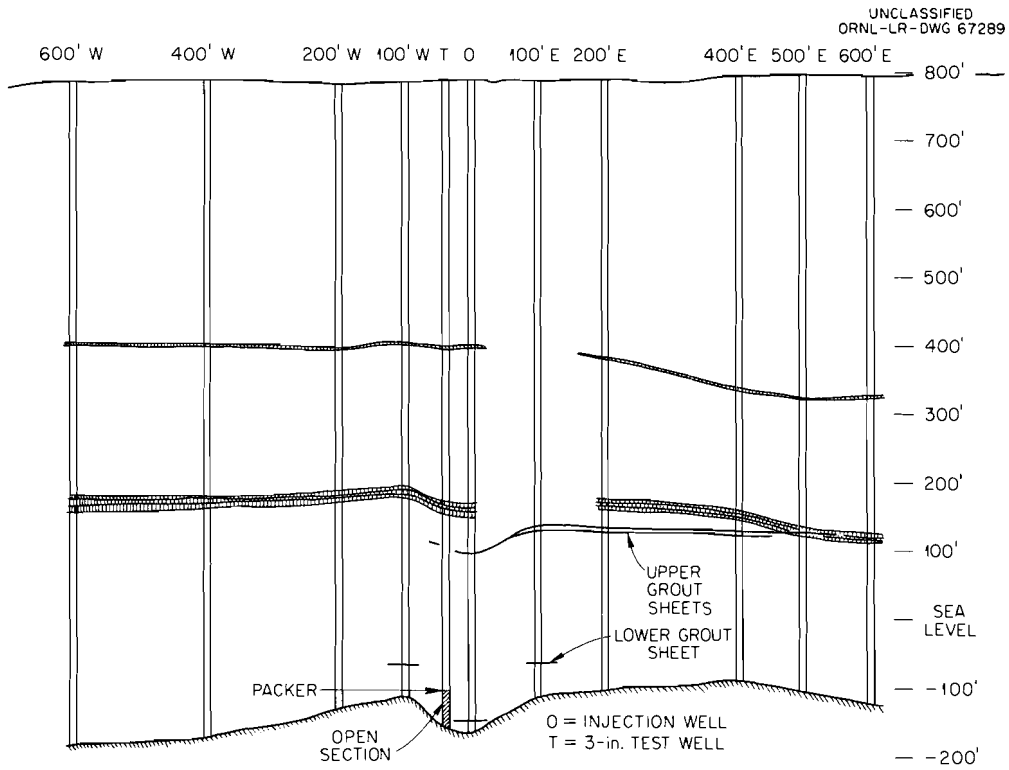


Fig. 5.5 East-west cross section showing approximate location of upper and lower grout sheets of second fracturing experiment.

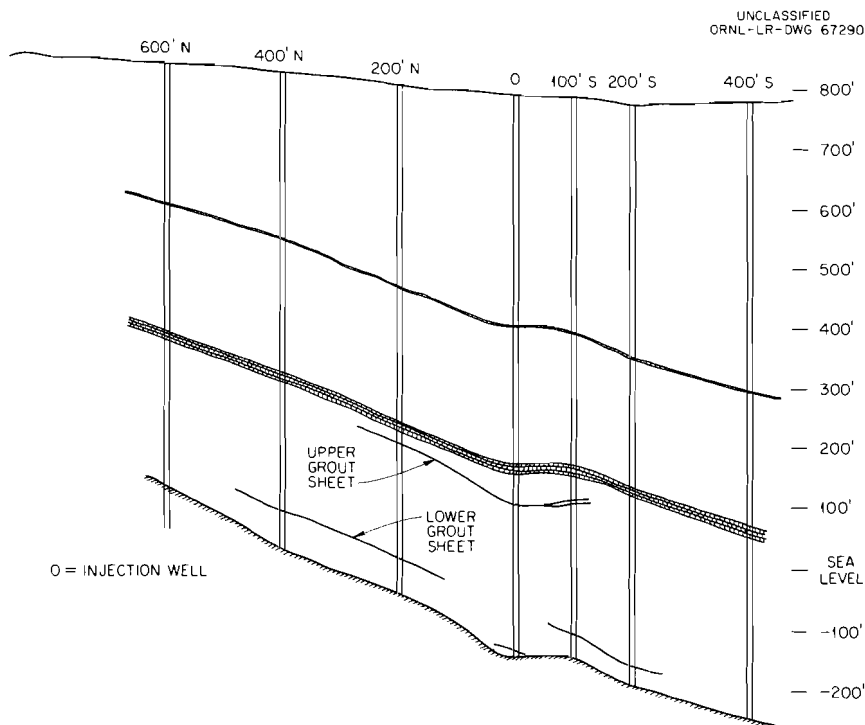


Fig. 5.6. North-south cross section showing approximate location of upper and lower grout sheets of second fracturing experiment.

At the time of the experiment, it was thought that the grout might make its way up the open-hole portion of the core hole as far as the packer at 892 ft and then break out laterally. The position of the packer is shown by an arrow on the east-west section (Fig. 5.5). However, this packer is only about 44 ft above the horizon at which the grout was injected, whereas the main extent of the lower grout sheet is about 80 ft above the level of injection. Movement up the open-hole portion of the core hole can therefore account for only about half the upward deflection of this grout sheet.

Extent of the Upper Grout Sheet. The upper grout sheet (Fig. 5.7) was found in wells 200 N, 200 NE, 300 NE, 400 NE, 100 E, 200 E, 400 E, 500 E, and 100 S. The grout sheet is not symmetrically distributed around the injection well, but extends much farther to the east and northeast than to the west. The cross sections suggest that the structure which confined the lower grout sheet also blocked the upper grout sheet from moving to the west, but that it was able to break through to the east. In breaking through it was also deflected upward about 30 to 40 ft, as seen in well 100 E. Farther east, in wells 200 E and 400 E, it was at or near this same new horizon, 20 to 25 ft below the center of the three beds of limestone. In well 500 E, it was at the center of the three beds of limestone but still at very nearly the same elevation. The three beds of limestone are folded or faulted downward about 25 ft between wells 400 E and 500 E. To the northeast, also, the upper grout sheet worked its way upward stratigraphically as it moved out, but not to any important extent.

The fracture formed was not, however, a single sheet. For example, in well 200 NE, there were three principal sheets and several minor sheets between 613.5 and 612.5 ft below land surface, and a fourth principal sheet at 607 ft. In well 300 NE there were four principal sheets in contact (Fig. 5.8), one against the other, and one of these was composed of two very similar layers. In well 200 E there was also good evidence of four principal sheets. The grout was not injected into the shale along a single fracture which continued to extend outward as pumping progressed, but rather as a series of fractures, probably one after the other, since the four (or five) separate layers in the core from well 300 NE (Fig. 5.8) show little tendency to intermix as they would if they had moved in concurrently. What actually happened is not known, but it is possible to make certain inferences. As the first sheet moved out into the shale, its leading edge must have lost some water to the shale and to minute fractures in the shale. Even though the shale is very impermeable, some fluid loss can be assumed, considering the large surface area passed over by the grout. The leading edge of the grout sheet may therefore have had a good chance of setting up by what is called a "screen out"; that is, by dehydration of the grout by loss of water to the formation. When this happened, the advance of the grout sheet was halted, and continued pumping initiated the formation of a new fracture back near the injection well.

The upper grout sheet area is about 245,000 ft<sup>2</sup>. Near the injection well, and at least as far out as well 300 NE, its total thickness is 0.040 ft, and in well 400 E its estimated thickness is 0.020 ft. If an average thickness of 0.030 ft is assumed, the volume of grout in place would be 7350 ft<sup>3</sup>. The cement used weighed 800,000 lb and would have taken up on setting 20 wt % water for a total weight of 960,000 lb. The

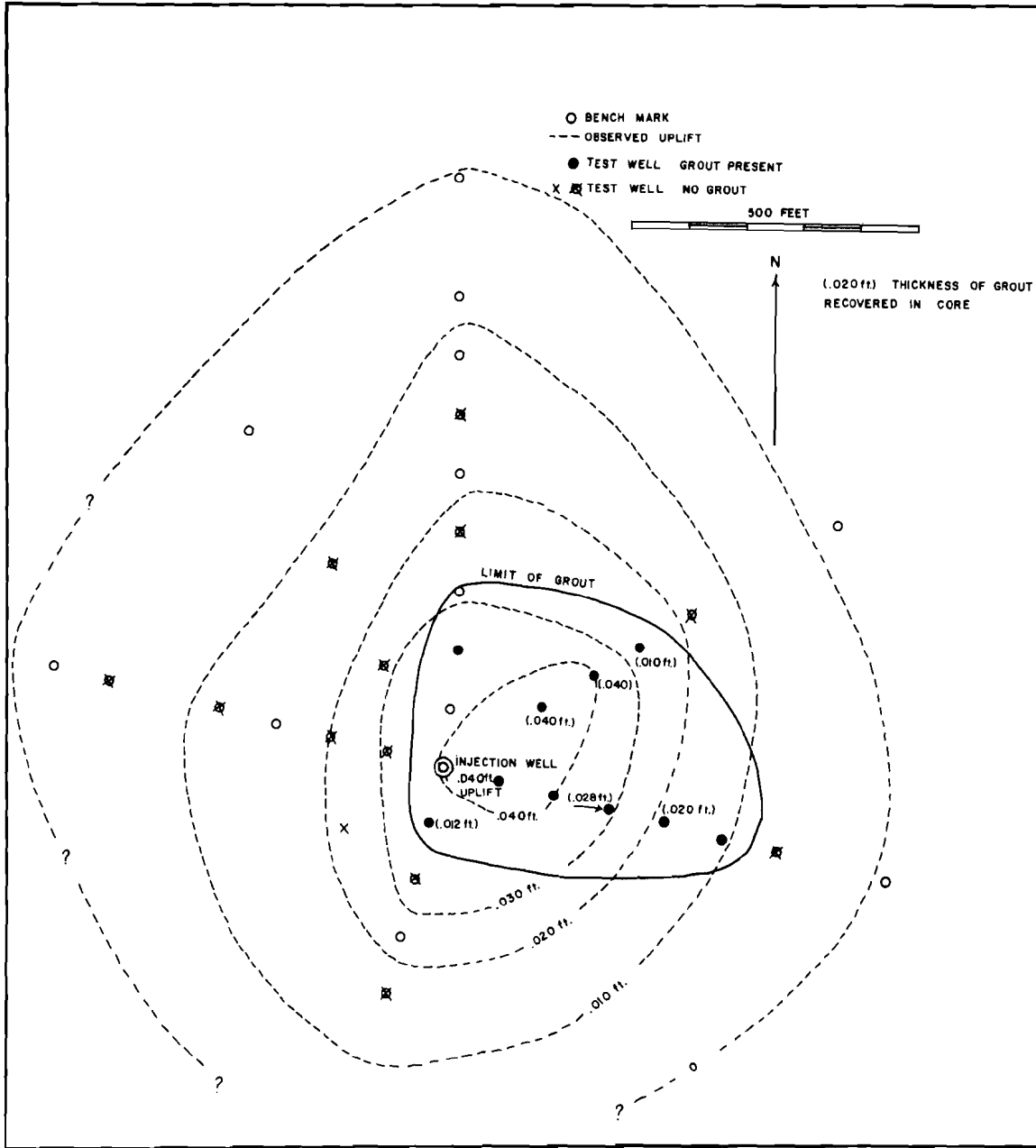


Fig. 5.7 Upper grout sheet of second fracturing experiment and observed uplift.

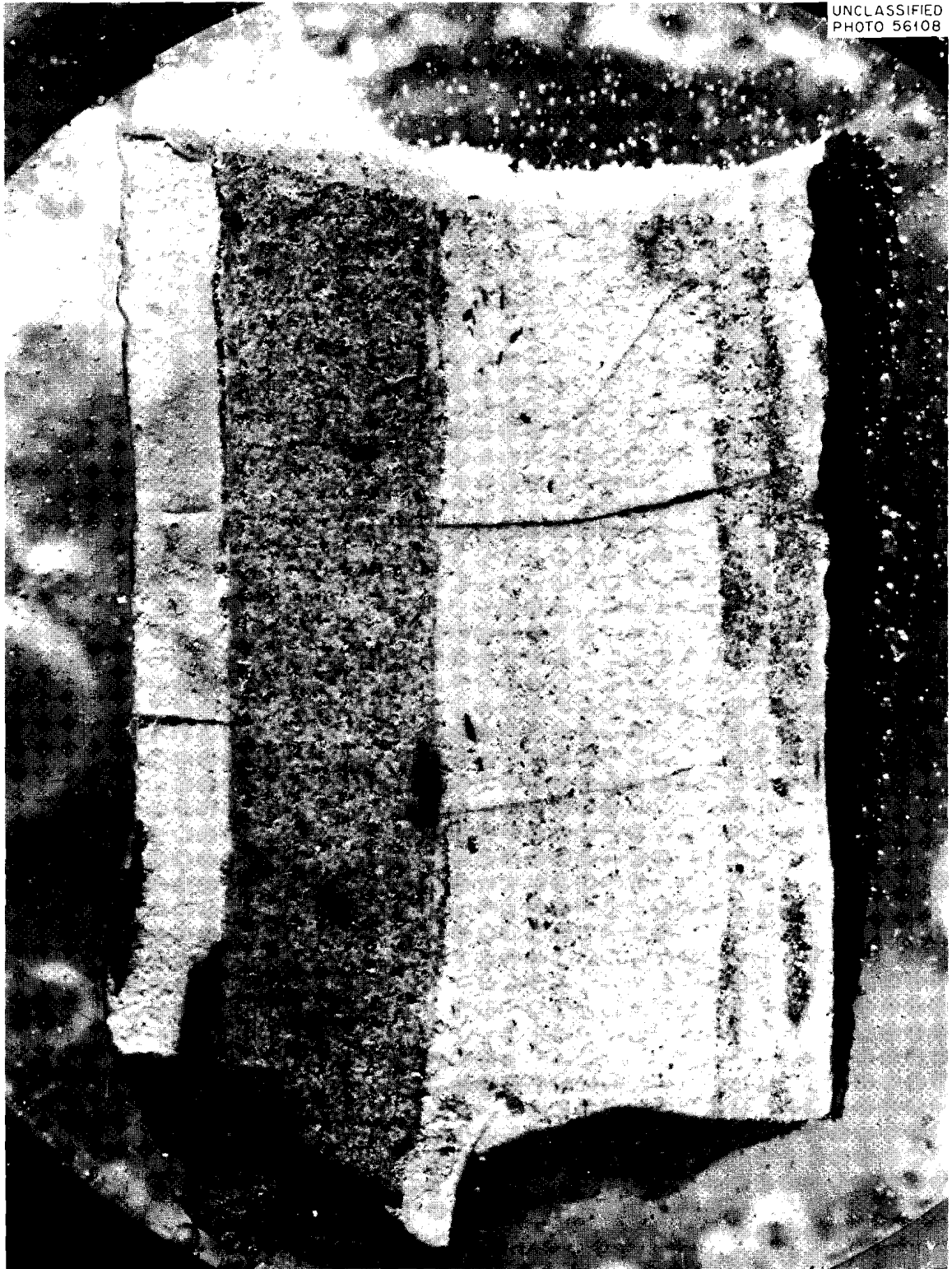


Fig. 5.8 Four (or five) layers that comprise the upper grout sheet 300 ft northeast of the injection well. Aggregate thickness is 0.5 in.

dried grout density is  $106 \text{ lb/ft}^3$ , which would give a volume of  $9000 \text{ ft}^3$ , somewhat more than the volume of  $7350 \text{ ft}^3$  suggested by drilling.

Surface Uplift. Figures 5.4 and 5.7 show the amount and extent of surface uplift, as determined by the observed relative displacements of the bench marks. The uplift in each case extends beyond the outer limits of the grout sheet. In the first injection, the general uplift, and in particular the more pronounced movement outlined by the 0.010-ft uplift contour, is to the east of the injection well, although the grout sheet is oriented north and south. The uplift produced by the second injection was both greater and more extensive than that due to the first, and the area of maximum uplift lay to the east of the injection well. It must be concluded that the pattern of uplift cannot be a guide to the underground position of the grout, except in so far as it suggests that a horizontal, rather than a vertical, fracture has been formed.

Too few cores containing grout were collected from the lower grout sheet to justify a comparison of aggregate grout thickness and amount of uplift; but, in the case of the upper grout sheet, the aggregate thickness of the grout layers in each well from which good cores were recovered corresponded closely with the amount of uplift observed at that point. In the case of the upper grout sheet, the following approximate values were obtained:  $45,000 \text{ ft}^2$  of land surface were uplifted 0.040 ft;  $123,000 \text{ ft}^2$  were uplifted 0.035 ft;  $190,000 \text{ ft}^2$  were uplifted 0.025 ft;  $450,000 \text{ ft}^2$  were uplifted 0.015 ft;  $752,000 \text{ ft}^2$  were uplifted 0.005 ft. This gives a total volume of surface displacement of  $21,460 \text{ ft}^3$ , compared to  $17,550 \text{ ft}^3$  of liquid grout injected. Clearly, the rock showed both shearing and tensile strength, not only because the uplift extended well beyond the area of the grout and because the volume of the uplift was greater than the volume injected, but also because the injection pressures were considerably greater than the weight of the overburden.

In the second injection, the pumping pressure at the surface was 2000 psi at a pumping rate of 200 gpm. At a greater depth and at a somewhat lower pumping rate, the friction loss was estimated at 450 psi. The pressure due to a 694-ft column of 12.5 lb/gal grout is also about 450 psi; therefore the pressure in the fracture was approximately 2000 psi, or  $288,000 \text{ lb/ft}^2$ . The work done in displacing  $17,750 \text{ ft}^3$  of grout into the fracture was therefore  $5.1 \times 10^9 \text{ ft-lb}$ . The volume of the uplift produced on the surface was  $21,460 \text{ ft}^3$ , and the work done in raising it was equivalent to lifting an area of  $21,460 \text{ ft}^2$  a vertical distance of 1 ft. As this block extends to an average depth of about 650 ft, and the rocks weigh close to  $144 \text{ lb/ft}^3$ , the work done in lifting the rock was only about  $2.08 \times 10^9 \text{ ft-lb}$ . Despite the large possible errors in the data and in the assumptions involved, it is apparent that the rock overlying the grout sheet was not passively uplifted, but that it had sufficient shearing and tensile strength to resist the deformations imposed on it. This is also shown by the high pumping pressures required and the area of surface uplifted.

Work Required to Complete the Second Experiment. Two more core wells will be completed to try to determine how and why the lower grout sheet was displaced upward some 80 ft before spreading out laterally. Several of the wells will be surveyed

with a photoclinoimeter and the structure sections redrawn if required. An attempt may be made to photograph the grout seam in several of the wells from which no core was obtained to determine its thickness. The material balance for amount injected and cement found in place should also be improved if possible. The bench marks may be surveyed again to see if there has been any settling of the land surface beyond the outer limits of the grout sheet.

## 5.2 Liquid Injection into Permeable Formations (D. G. Jacobs)

The use of wells to dispose of brine to deep permeable formations is a current practice in the petroleum industry. Of the additional factors to be considered for the disposal of radioactive liquids, the most significant are those which concern the safety of the method and the additional costs because of the safety requirements. The safety aspect can be resolved into two problems: (1) radiation exposure to personnel and surface contamination due to handling of radioactive liquids at the disposal site, and (2) environmental contamination due to movement of the radionuclides in the disposal formation. The first problem is encountered in every scheme for handling radioactive liquids, and the techniques for evaluating and controlling these hazards have a firm basis. However, in order to assess the hazards associated with environmental contamination, one must be able to predict the movement of the radionuclides in the environment.

In the environment radionuclides move along the same stream lines as the transporting solution but are retarded in movement by sorptive processes in the disposal formation. Movement of the radionuclides can be predicted by describing the movement of water in the formation and correcting for sorptive processes.

### 5.2.1 Sodium-Calcium-Strontium Exchange

Samples of Richfield sand were obtained from W. J. Kaufman and Y. Inoue, University of California. The exchange capacity was determined in triplicate by saturating a 75-g column with neutral 1 M  $\text{CaCl}_2$ , washing free of chlorides, and leaching with neutral 1 M sodium acetate in 50-ml increments until no further calcium was removed. Calcium in the effluent, as determined by titration with EDTA, showed an average exchange capacity of 2.96 meq/100 g.

In the study of Na-Ca-Sr exchange, the columns were presaturated with 0.005 M  $\text{Ca}(\text{NO}_3)_2$  solution containing various concentrations of  $\text{NaNO}_3$ . The columns were subsequently saturated with chloride solutions of the same cationic composition to which was added Sr-85 ( $\sim 2 \times 10^{-8}$  M  $\text{SrCl}_2$ ). The effluent was sampled at 25-ml intervals and counted for Sr-85. After saturation, the calcium and strontium were removed by leaching the column with neutral 1 M sodium acetate. Aliquots of the eluate were counted for Sr-85, and samples were analyzed for calcium by EDTA titration. Leaching continued until the columns were depleted of calcium and strontium. The results of these experiments, corrected for pore volume, show that strontium is selectively sorbed over calcium by a factor of  $\sim 1.1$ , while the selectivity for calcium over sodium (at pH 7) is  $\sim 50$  g/ml (Table 5.1). From these experiments a value of 4.27 meq/100 g was obtained for the exchange capacity.

Table 5.1 Sodium-Calcium-Strontium Exchange on Richfield Sand

$(Ca^{++}) = 0.005 \underline{M}$ ;  $(Sr^{++}) = 2 \times 10^{-8} \underline{M}$

Na Conc (M)	Column 1		Column 2		Column 3		Average			
	$(K_d)_{Sr}$ (ml/g)	$(K_d)_{Ca}$ (ml/g)	$(K_d)_{Sr}$ (ml/g)	$(K_d)_{Ca}$ (ml/g)	$(K_d)_{Sr}$ (ml/g)	$(K_d)_{Ca}$ (ml/g)	$(K_d)_{Sr}$ (ml/g)	$(K_d)_{Ca}$ (ml/g)	$K_{Sr/Ca}$	$K_{Ca/Na}$ (g/ml)
0.000	4.23	4.37	4.12	4.53	4.36	3.90	4.24	4.27	0.99	--
0.005	4.49	4.39	4.27	4.09	4.49	3.82	4.42	4.10	1.08	35.5
0.05	3.60	3.35	3.29	3.25	3.72	3.33	3.54	3.31	1.07	90.1
0.5	0.36	0.28	0.33	0.27	0.43	0.39	0.37	0.31	1.19	49.5

Kaufman et al.(13) found a mean exchange capacity of 2.51 meq/100 g for the Richfield sand and a selectivity factor for strontium over calcium of 1.65 in 0.005 M CaCl<sub>2</sub>. Although his value for the exchange capacity is considerably lower, his value for the strontium K<sub>d</sub>, 4.14 ml/g, compares very well with our value of 4.24 ml/g in a solution of the same concentration. His low value for exchange capacity may be due to a hydrocarbon coating on the exchanger material, as we experienced difficulty in wetting the original sample and noted an increase in exchange capacity with continued cycles of saturation and leaching. It is felt that the selectivity factors obtained here are likely to be more accurate, as calcium and strontium were determined in the same sample.

The selective sorption of strontium over calcium on Richfield sand agrees with observations of strontium-calcium exchange on reference clay minerals (Table 5.2). Divalent-exchange studies, made with Conasauga shale, indicated that the preference of the cation-exchange surface for strontium over other alkaline earth cations decreases with decreasing size of the hydrated ion. The selectivity of calcium over sodium is also of the same order of magnitude for Richfield sand as for the strontium to sodium selectivity of reference clays.

Table 5.2 Strontium Exchange Properties of Various Clay Minerals

Mineral	K <sub>Mg</sub> <sup>Sr</sup>	K <sub>Ca</sub> <sup>Sr</sup>	K <sub>Ba</sub> <sup>Sr</sup>	K <sub>Na</sub> <sup>Sr</sup> (g/ml)
Vermiculite	--	1.31 ± 0.16	--	48 ± 9
Fithian illite	--	1.19 ± 0.17	--	91 ± 15
Kaolinite	--	1.21 ± 0.19	--	57 ± 11
Wyoming bentonite	--	1.33 ± 0.29	--	--
Arizona bentonite	--	1.26 ± 0.15	--	--
Conasauga shale	1.44 ± 0.14	1.24 ± 0.06	1.00 ± 0.26	--

### 5.2.2 Comparison of Chloride and Strontium Breakthrough Curves

Because anions are not actively sorbed by cation exchangers, they can be used to measure the dispersion of solution passing through a cation-exchange column. In these experiments, chloride was determined in the effluent as the nitrate solution was displaced by chloride solution. It is seen that the strontium breakthrough curve can be predicted on the basis of dispersion of the solution in the column (Fig. 5.9). This implies that radionuclide breakthrough at a particular point in the environment can be predicted by observing the breakthrough of a water tracer and correcting for the sorptive properties of the formation for the radionuclide in question.

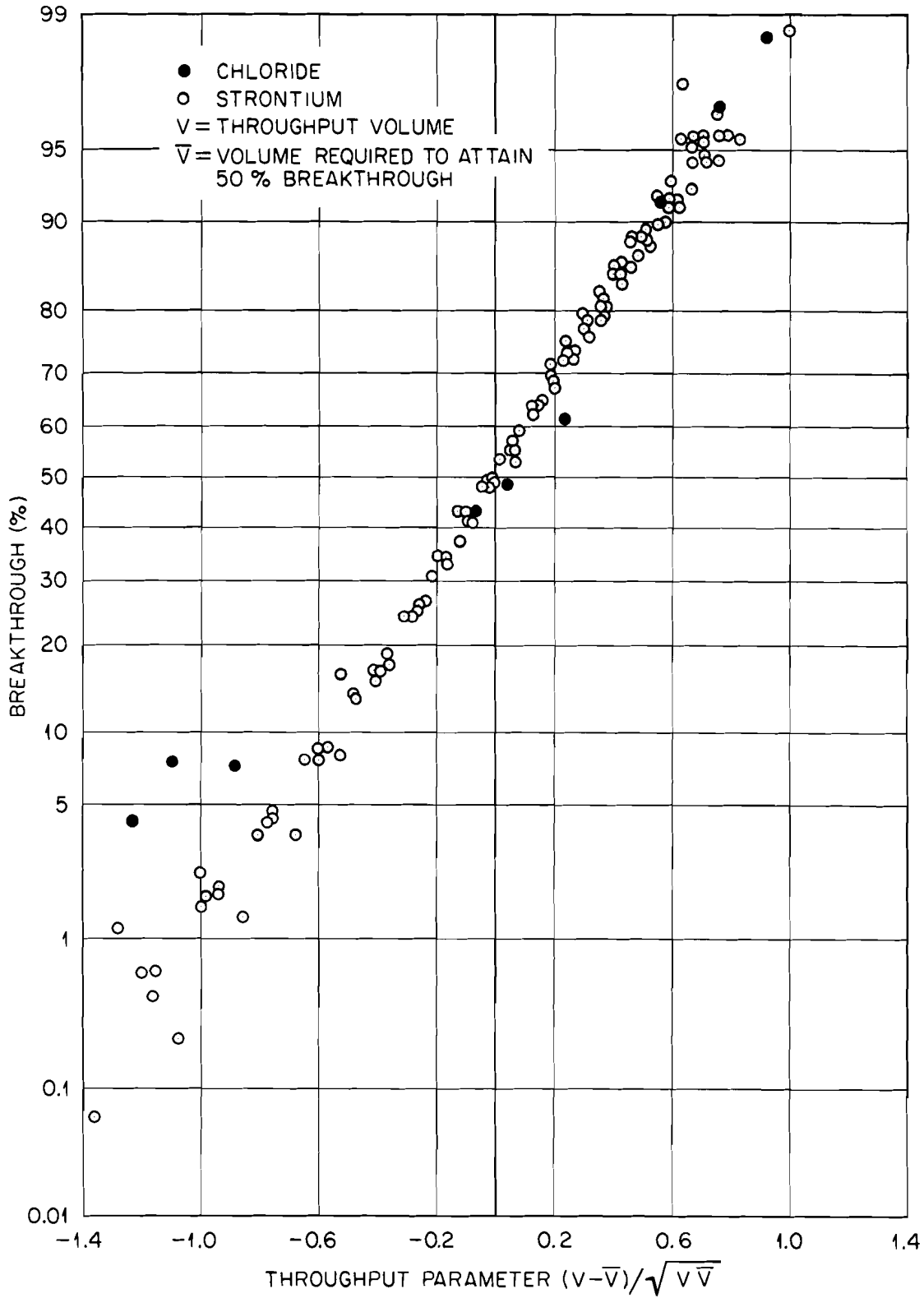


Fig. 5.9 Comparison of chloride and strontium breakthrough curves.

## 6.0 DISPOSAL IN NATURAL SALT FORMATIONS

### 6.1 Field Tests (R. L. Bradshaw and F. M. Empson)

The design of an experiment to determine the effect of temperatures greater than 250°C on salt in situ was discussed previously (2). Figure 6.1 shows the experiment in plan and in elevation as actually constructed. Holes in the floor of the Carey Mine at Hutchinson were drilled with extreme care to develop them as straight and as nearly vertical as possible. Both the 8- and 1-3/16-in. holes were drilled with diamond core bits, using brine as the drilling fluid, a fixed vertical guide rod, and low drilling speeds.

The diameter of the 7-7/8-in.-dia heater hole, calipered with a dial gage that read to 0.001 in., was found to be 7.820-7.900 in., averaging 7.875 in. Measurements at 60° intervals did not indicate any eccentricity with orientation. Therefore insertion of a 6-5/8-in. stainless steel pipe, containing the heating elements, left an annular air space approximately 5/8 in. wide. The straightness of the hole was shown qualitatively by a straight edge held against its surface. The straightness of the 1-3/16-in. thermocouple holes was shown by lowering a small light source to the bottom. No evidence of bending or irregularity was seen. The entire wall surface was visible, and there were no breaks in the salt surface.

The departure from vertical of the 7-7/8-in. heater hole was measured by placing a scale at the bottom of the hole and hanging a plumb bob from the level of the floor down the center of the hole. Displacement of the scale at three positions, in reference to the plumb bob, indicated that the bottom of the hole was 0.63 in. to the east of the top of the hole. Alignment of the 1-3/16-in. thermocouple holes was determined by inserting a snug wooden rod extending several feet above the floor level. Lateral deviation of the wooden rod, in a fixed vertical distance, was observed with a transit from two points, 90° apart, and was used to compute the exact location of the thermocouples in the hole.

The thermocouples and cylindrical heater (stainless steel pipe, 5-ft long x 6-5/8 in. o.d., electrically heated in the lower 4 ft) were installed and the heater was turned on Jan. 27, 1962. The experiment was terminated after 3-1/2 days' operation due to the presence in the annulus around the heater of water, presumably absorbed by the shale during drilling. After 70 hr operation, the water level was ~6 in. below the top of the cylindrical heater, and the water was boiling. After 84 hr operation, the annulus around the heater was filled with crystals, apparently recrystallized salt dissolved from the wall of the hole.

The highest measured salt temperature was 127°C (106°C rise) at a distance of 9.6 in. from the center of the heater (Fig. 6.2). Although not measured, the maximum salt temperature at the inner surface of the hole (4 in. from heater center) was estimated to be about 200°C. Also shown in Fig. 6.2 are theoretical curves with thermal conductivity and diffusivity adjusted so that the 9.6-in. curve coincides with the experimental points for a temperature rise from 50 to 105°C. The conductivity

UNCLASSIFIED  
ORNL-LR-DWG 67292

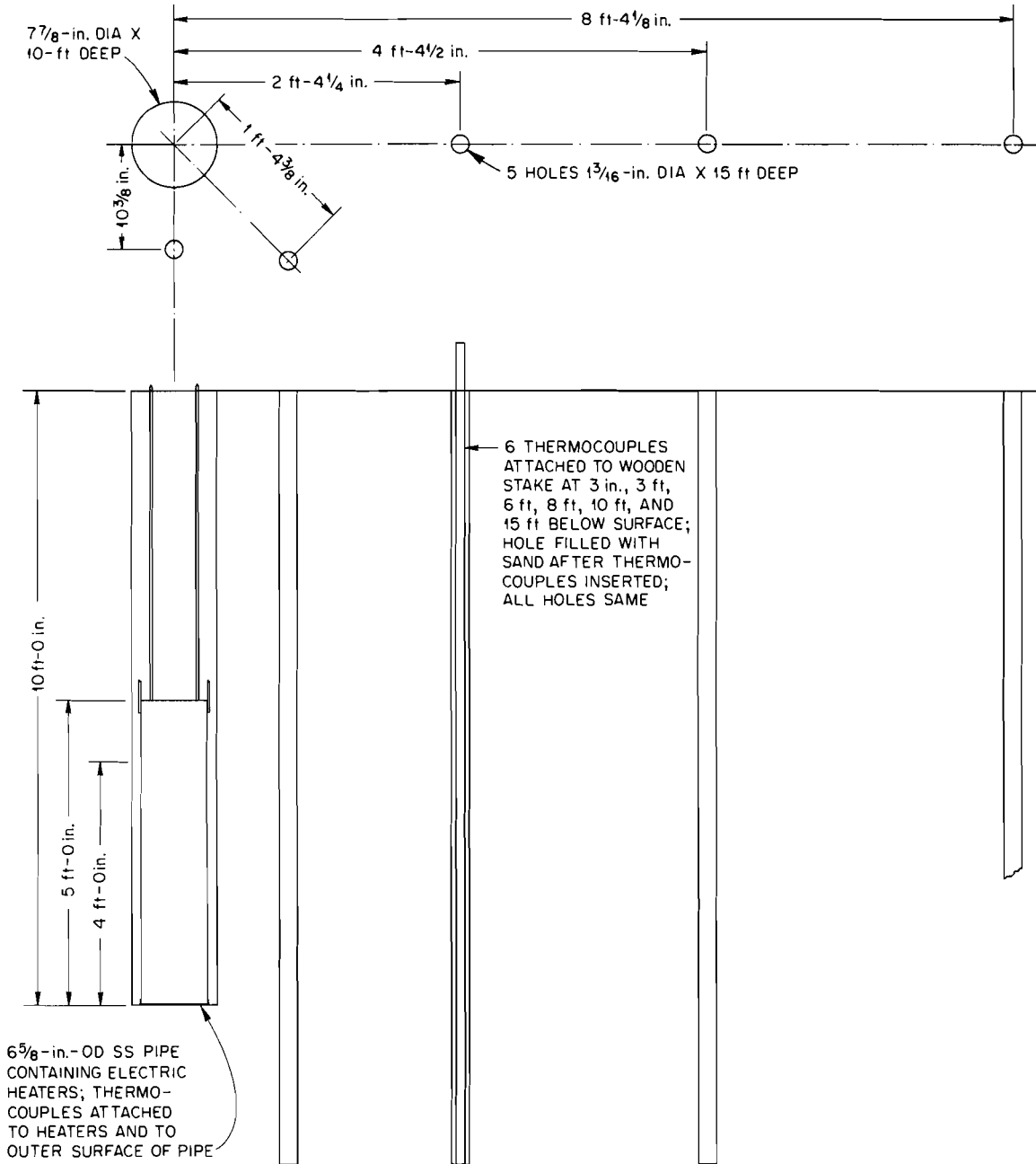


Fig. 6.1 High-temperature experiment.

determined in this way was 2.7 Btu/hr.ft.°F (single crystal value for 70°C) and diffusivity was 0.08 ft<sup>2</sup>/hr (130°C value).

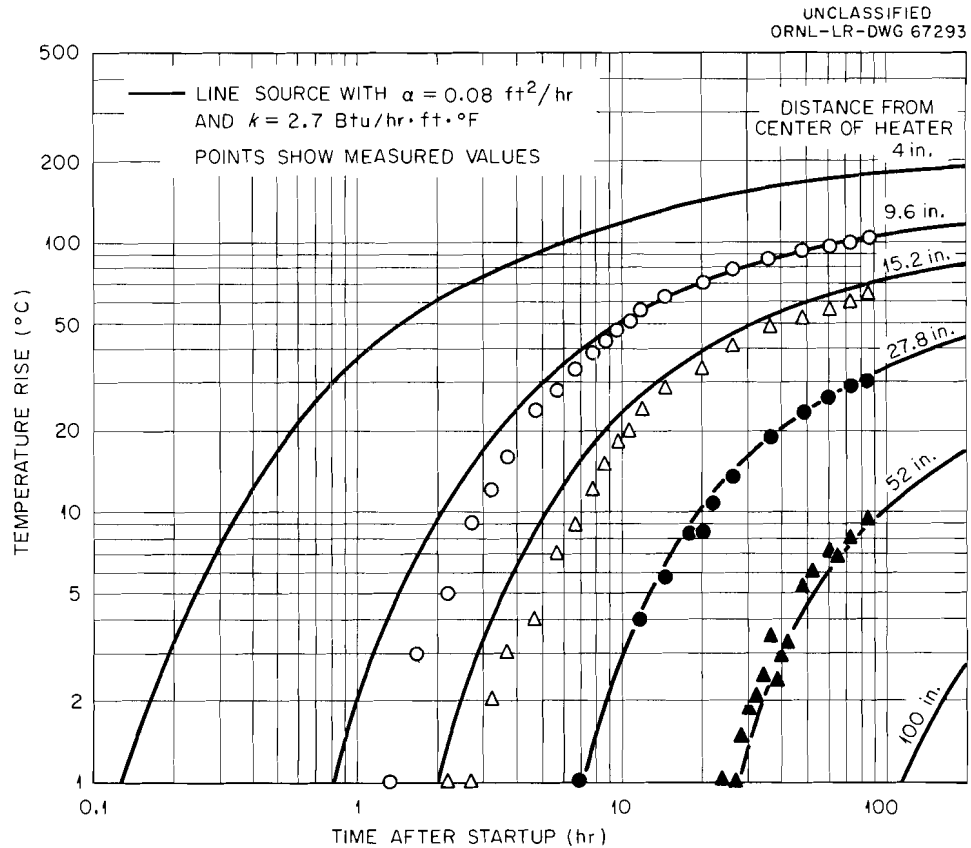


Fig. 6.2 Comparison of temperature rise in high temperature cylinder test 1 with theoretical for line source. Heater was 6 in. dia by 4 ft; power input = 3100 watts.

### 6.2 Laboratory Study of High-Temperature Effects (H. Kubota)

The effect of elevated temperature on salt was investigated in connection with the proposed storage of pot-calcined wastes in natural salt formations. Lumps of salt weighing 300-800 g, in the form of core drillings or pieces from mining operations in the Carey Mine at Hutchinson, were used. In each of six tests, the salt mass shattered and ruptured the metal basket used to contain the salt when the temperature reached 260 to 280°C. This effect was observed in the same temperature range regardless of the rate of heating. The shattered salt consists of crystals varying from about 10 mesh to over 1 in. in size. Three possible causes have been advanced for this phenomenon: (1) unequal strain resulting from unequal expansion along the different crystal axes, (2) oxidation of occluded organic material, or (3) pressurization of trapped water. It seems improbable that No. 1 is the cause, since the salt shattered with about the same degree of violence and at the same temperature no matter how slowly the temperature was raised.

When the heating was performed in a bomb, a cloud of steam was observed coincident with the disintegration. Analysis of the gas in the bomb showed small amounts of carbon dioxide and carbon monoxide. The amount of water released was at least an order of magnitude greater than that of the carbon oxides. At present, therefore, it is thought that the pressurization of the trapped water was also partially responsible for the fracturing.

### 6.3 Plastic Flow Studies (W. J. Boegly, Jr.)

Theoretical analyses of the stresses around salt mine openings, the extent of the plastic zone, and the rate and amount of flow resulting from the plastic zone were initiated by R. E. Glover of Denver, Colorado, a consultant. He is also calculating the effects of temperature on the "close-in" movement (plastic flow due to thermal stresses and thermal expansion) near cylindrical holes containing radioactive solids in the floor of a salt mine.

In order to evaluate and assist in these calculations, it will be necessary to make field measurements of the stresses around mine openings. A number of methods for stress measurement are available; however, they have been applied mainly to "hard" rocks, and their applicability to very plastic rocks must be determined. The most promising of these is the concentric borehole method, currently used by the U. S. Bureau of Mines (14), in which a small-diameter borehole is drilled into the rock and a borehole deformation gage is inserted. Next, a larger diameter hole is drilled around the borehole gage, and the deformation of the inner borehole after stress relief is measured. From these values and Young's modulus, the stress can be calculated. The values of stress obtained by this procedure check quite well with the expected stresses, provided the correct value of Young's modulus is used. Since the value obtained for Young's modulus is dependent on the test method, sample size, sample age, and various other factors, a standardized technique for determination of this plastic property is required, and studies on this are being started.

## 7.0 CLINCH RIVER STUDY

### 7.1 Dispersion Studies (P. H. Carrigan\* and B. J. Frederick\*\*)

On Feb. 1, 1962, 10 curies of Au-198, 5500 times the MPC<sub>w</sub>, was discharged into the mouth of White Oak Creek over a period of 80 sec; the movement of gold was monitored in the Clinch River to Centers Ferry, 16.3 miles downstream.

---

\* On loan from Tennessee District, Surface Water Branch, Water Resources Division, U. S. Geological Survey.

\*\* Research Section, Surface Water Branch, Water Resources Division, U. S. Geological Survey.

Because of turbulent diffusion, the peak concentration of Au-198 decreased as the radioactive "cloud" moved downstream. The variation in peak concentration with distance is shown in Fig. 7.1a. Downstream from Clinch River Mile 16 (CRM 16) the dispersion was largely in the longitudinal direction. Therefore, the rate of change in peak concentration with distance was much less than for upstream reaches.

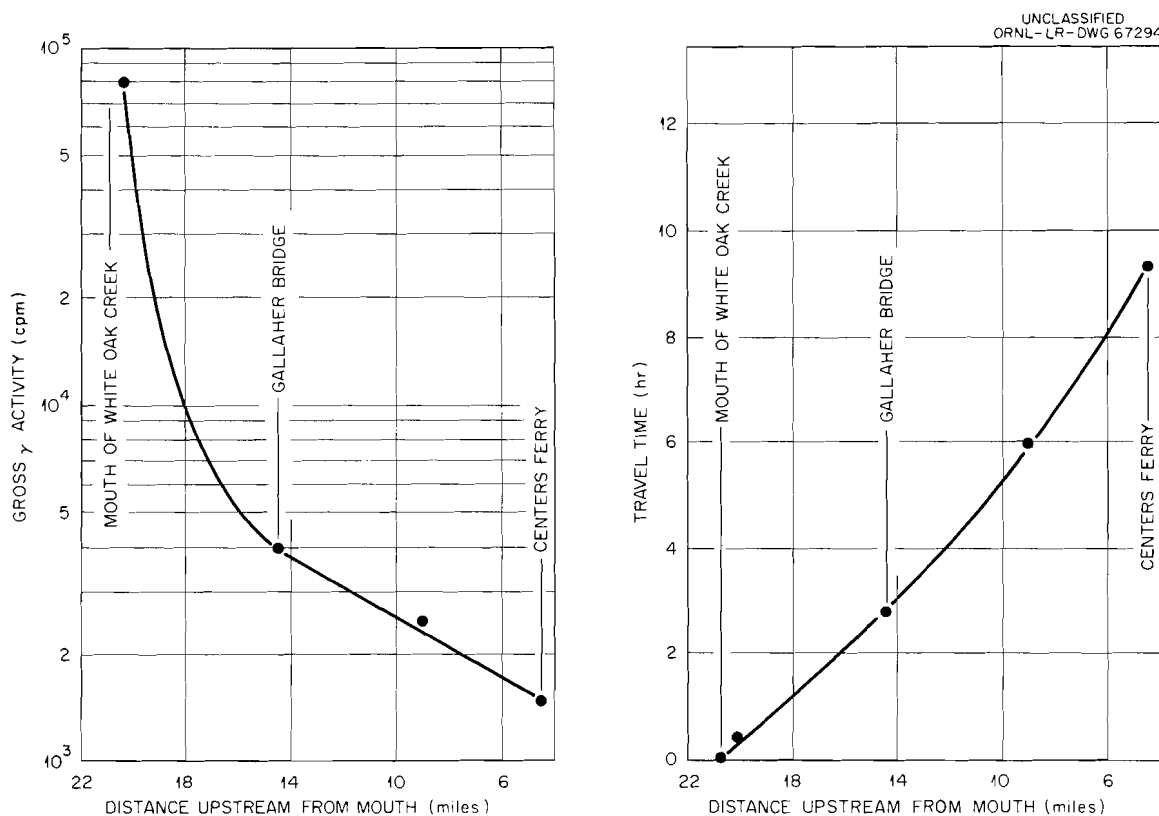


Fig. 7.1 Variation of (a) maximum concentration of Au-198 radioactivity and (b) time of travel with distance in Clinch River. Tracer study of Feb. 1, 1962.

The time of travel for the peak concentration from the mouth of White Oak Creek (CRM 20.8) to Gallaher Bridge (CRM 14.5) at the intake to the ORGDP water plant was 2.8 hr (Fig. 7.1b), and the concentration of Au-198 in this section was about 15% of the  $MPC_w$ . The time of travel for the peak concentration from White Oak Creek to Centers Ferry (CRM 4.5), 9.3 hr, is about 10% less than that predicted by TVA (15).

Frequently during summer months, power releases are made once daily from Norris Reservoir. The variation in flow of the Clinch River above Centers Ferry (CRM 4.5) produced by such a release during a 24-hr period is shown in Fig. 7.2a. The effect of these power releases on radioactivity levels in the Clinch above Centers Ferry was shown by analysis of water samples collected at 2-hr intervals. For several days prior to the test period, the variation in daily discharge at Norris

Dam was the same as for the test. The discharge of radioactivity from White Oak Creek decreased gradually during the same period (Fig. 7.2b).

Generation of electric power at Melton Hill Dam is scheduled to begin the latter half of 1963. The release of water used to generate power will cause daily variations in the water level of the Clinch River. As a result of a maximum release of 23,000 cfs immediately downstream from White Oak Dam, the backwater from the Clinch will raise the level of White Oak Creek from el. 741.0 ft to el. 744.5 ft in the summer and from el. 735.0 ft to el. 742.7 ft in the winter (16). The magnitude and deviation of these daily releases from Melton Hill Reservoir are shown in Fig. 7.3.

As a consequence of this backwater, an increase in the surface area of White Oak Lake is possible. The increase in area, without diversion of White Oak Creek around the lake, will depend on the water level of the Clinch River, the duration of backwater, the level of gate crests in White Oak Dam, and the inflow of White Oak Creek to the lake. An estimate of lake inundation for three conditions of gate operation at White Oak Dam is shown in Fig. 7.4.

## 7.2 Analysis of Clinch River Water and Sediments (R. M. Richardson and R. J. Pickering\*)

Analyses of Clinch River water and sediments have been reviewed preliminary to tabulation and interpretation of the accumulated data. A period of high Ru-106 activity at water-sampling stations is believed to be the result of washing out of accumulated nonlocal atmospheric fallout during a period of heavy rainfall following a period during which concentrations of radioactivity in the air were slightly higher than normal. A program for submitting check samples for correlation of analyses between different laboratories is being planned.

On Jan. 31, 1962, water-sampling equipment was installed at the pump house of ORGDP by the U. S. Public Health Service. The responsibility for servicing the equipment has been assumed by personnel of the U. S. Geological Survey.

## 8.0 FUNDAMENTAL STUDIES OF MINERALS

(T. Tamura)

The presence of sodium nitrate in waste solution increases the removal of strontium by a calcite column (17), but decreases strontium removal by a rock phosphate column. In either system, the material beneficial for strontium removal is calcium phosphate. Based on experiments described below, a tentative hypothesis is suggested for the role of sodium nitrate: In a calcite column calcium released by the sodium reacts with soluble phosphate in the waste to form insoluble calcium

---

\* On loan from Tennessee District, Surface Water Branch, Water Resources Division, U. S. Geological Survey.

UNCLASSIFIED  
ORNL-LR-DWG 67295

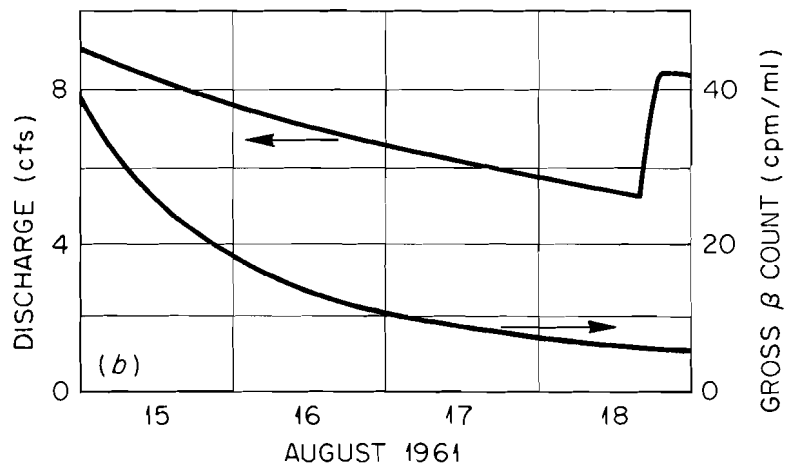
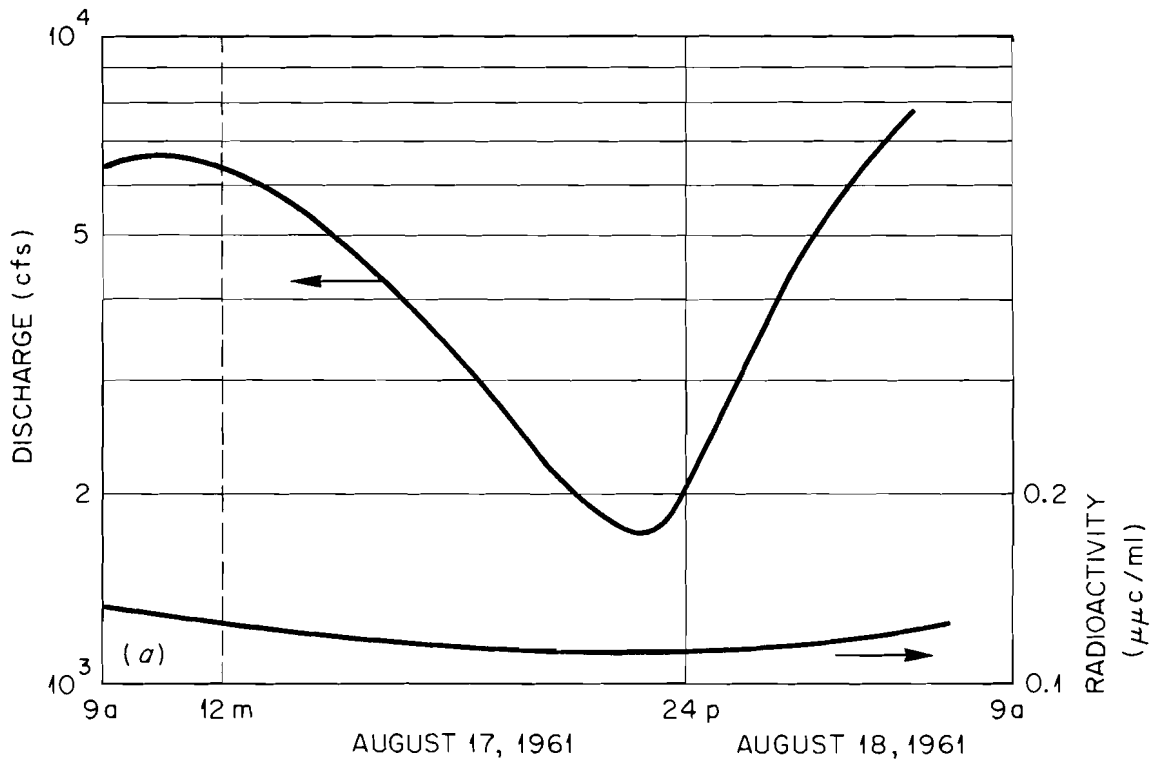


Fig. 7.2 Variation in discharge and concentration of radionuclides in (a) Clinch River during a 24-hr period and (b) in White Oak Creek during a 4-day period.

UNCLASSIFIED  
ORNL-LR-DWG 65384

NOTE: THE AVERAGE WEEKLY INFLOWS OF 2900, 6000, AND 8000 cfs ARE THOSE EXPECTED TO BE EQUALED OR EXCEEDED ABOUT 90%, 50% AND 30% OF THE TIME, RESPECTIVELY DURING THE WINTER MONTHS.

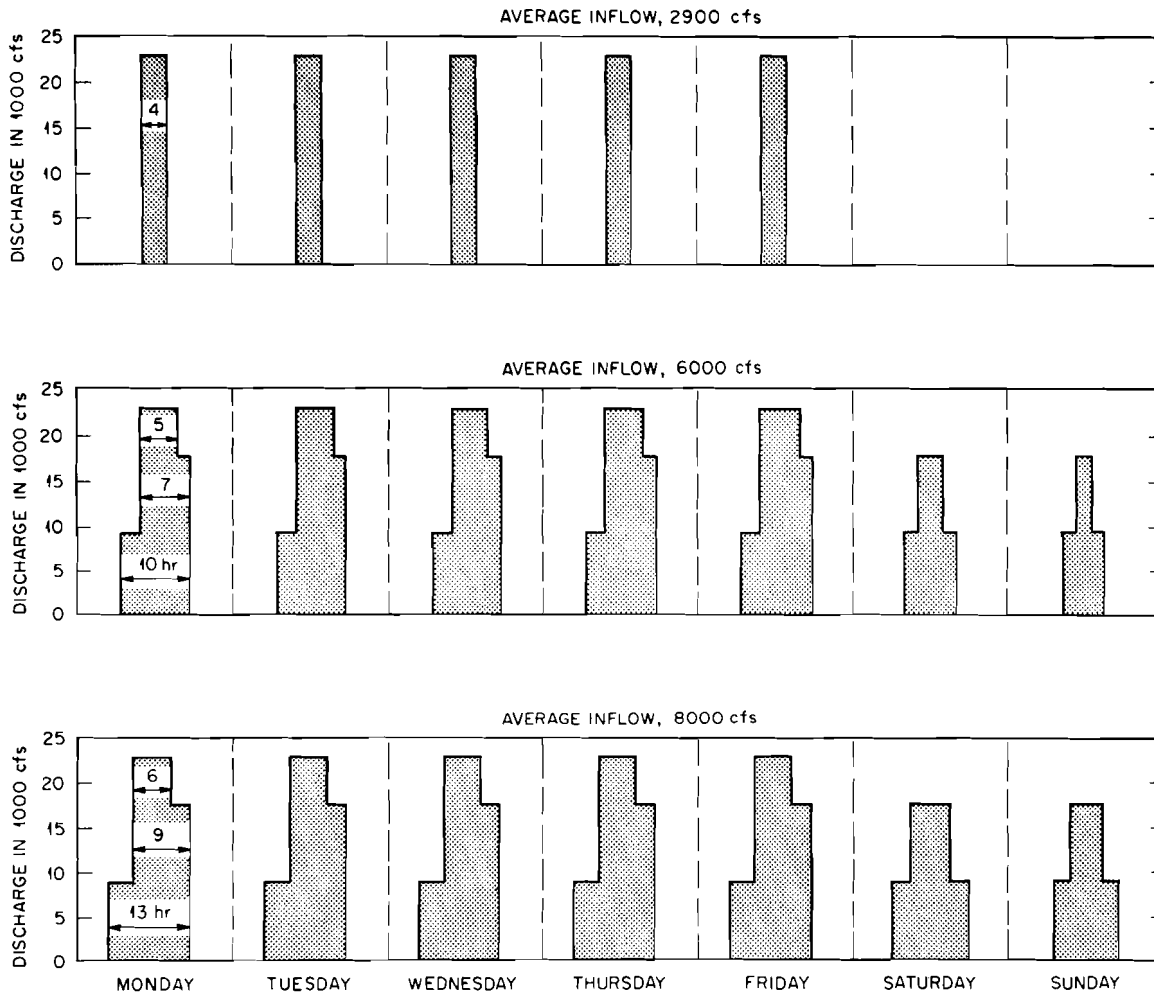


Fig. 7.3 Possible schedule of releases from Melton Hill reservoir for average weekly inflows to the reservoir.

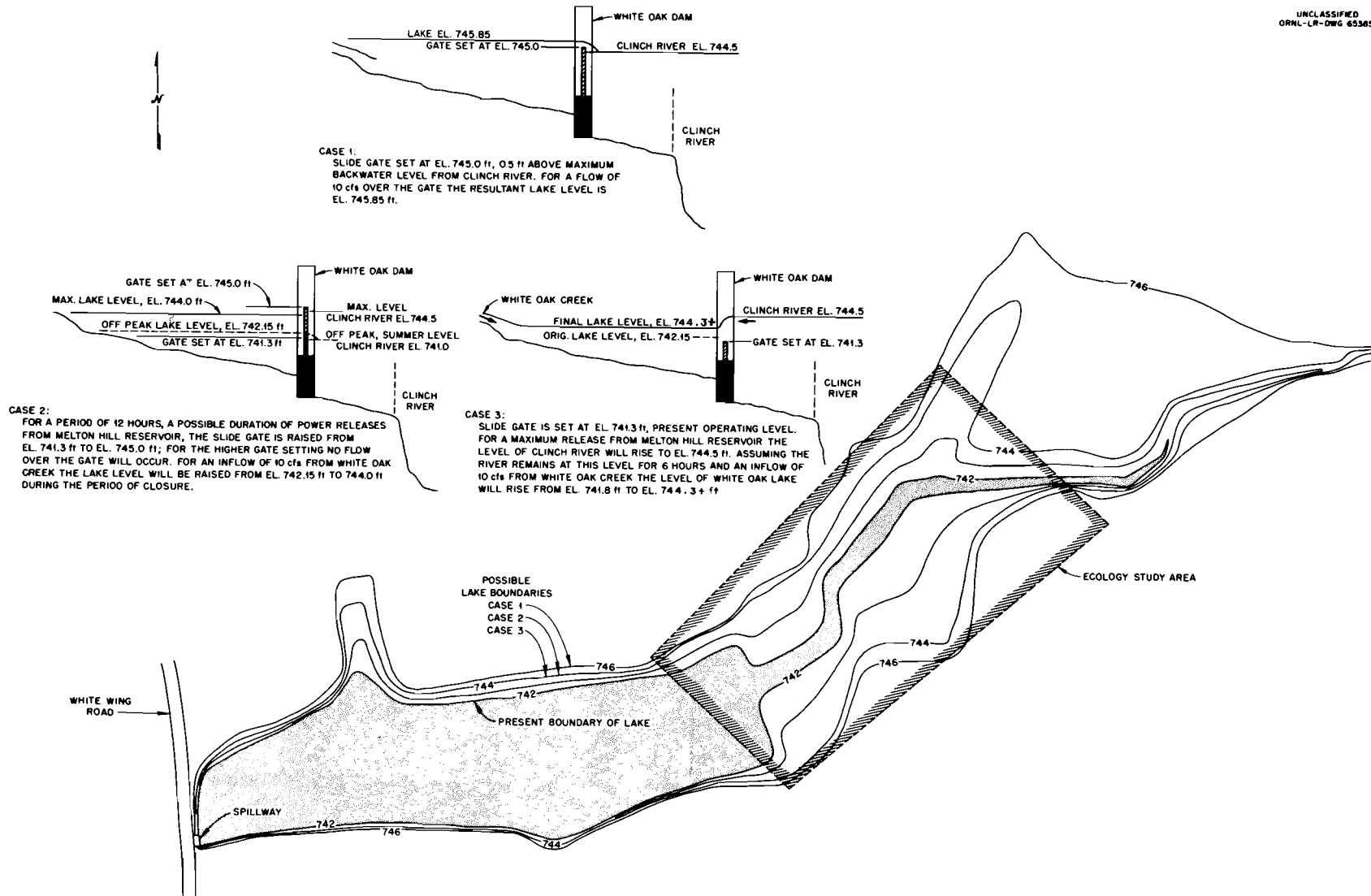


Fig. 7.4 Possible limits of inundation of White Oak Lake.

phosphate. If the phosphate concentration is in great excess, as is usually the case, the calcium would not be expected to compete with strontium for the phosphate; rather, increases in calcium concentration would favor the formation of larger amounts of calcium phosphate. In a rock phosphate column, the matrix is calcium phosphate (apatite). The released calcium does not form an insoluble reaction product with the waste solution, and the added sodium ions compete with strontium and calcium for exchange sites on the apatite.

In the experiments described below a known weight of mineral was contacted with either demineralized water or sodium nitrate solution in a stoppered vial. After being shaken for a predetermined time in a Burrell "wrist-action" shaker, the vial was centrifuged 2 min and an aliquot of the solution was titrated for calcium with Versene-eriochrome Black T, using a microburet.

### 8.1 Dissolution of Calcium from Calcite

More titratable calcium was released from calcite by 0.5 M NaNO<sub>3</sub> solution than by demineralized water (Table 8.1). That the difference was not due to titrating the calcium in different media was shown by the consistent calcium values obtained in analyses of calcium standards made up in demineralized water and sodium nitrate solution. The solubility of calcite is 0.0014 g/100 g of water at 25°C, or 0.28 meq of calcium per liter (18), and the amounts determined in demineralized water in these tests agreed closely. The particle size of the calcite had no effect on the results.

The results with different solvent contact times indicated that equilibrium is attained rapidly and that 15 min contact is sufficient for equilibration (Table 8.1). The difference in calcium solubility in demineralized water and sodium nitrate solution existed with all contact times tested.

Increasing the sodium nitrate concentration from 0.1 to 5.0 M increased the dissolved calcium from 0.70 to 1.13 meq/liter (Table 8.1). Calcium solubility was slightly higher in demineralized water in this series than in the earlier series, but these higher values are attributed to experimental error. That they were not totally due to dissolved CO<sub>2</sub> was shown with demineralized water that had been boiled, stoppered, cooled, and kept free from atmospheric CO<sub>2</sub> during contact with the calcite. This water dissolved ~10% less calcium, with calcium concentrations of the order of 0.28 mN. The constancy of the calcium concentrations in successive leaches suggests that the dissolution involves the entire calcite particle and not merely a surface reaction.

### 8.2 Dissolution of Calcium from Rock Phosphate

Tests with rock phosphate are still in progress, but preliminary results (Table 8.1) indicate differences in the response of calcite and rock phosphate. As with calcite, more calcium was dissolved in the presence of sodium nitrate, but unlike calcite, particle size and successive leachings strongly affected the results. Less calcium

Table 8.1 Dissolution of Calcium from Calcite and Rock Phosphate by Demineralized Water and Sodium Nitrate Solution

Particle Size (mm)	Contact Time (min)	Ca Dissolved by Demineralized H <sub>2</sub> O (meq/liter)		Conc (M)	NaNO <sub>3</sub> Soln Ca Dissolved (meq/liter)		
		1st Leach	2nd Leach		1st Leach	2nd Leach	3rd Leach
Calcite							
0.5-0.25	30	0.33		0.5	1.1		
0.25-0.10		0.27			1.1		
0.10-0.05		0.27			1.1		
< 0.05		0.27			1.2		
0.5-0.25	15	0.28		1	1.05		
	30	0.28			1.01		
	60	0.29			1.13		
	300	0.29			1.16		
0.5-0.25	15	0.41	0.34	0.1	0.70	0.66	0.64
				0.5	0.98	0.94	1.05
				1.0	1.18	1.12	1.07
				5.0	1.13	--	--
Rock Phosphate							
0.5-0.25	30	0.08		0.5	0.40		
0.25-0.10		0.12			0.49		
0.10-0.05		0.33			1.04		
< 0.05		--					
0.5-0.25	30			1.0	0.61	0.24	0.20
0.25-0.10					0.75	0.28	0.24
0.10-0.05					1.31	0.54	0.37
< 0.05					1.97	0.79	0.50

was dissolved with successive leachings, suggesting that the high initial calcium concentration is caused by the presence of some very fine particles in each size range. The increase in calcium concentration with decrease in particle size supports this explanation. There was some indication that the sodium nitrate concentration affected the rock phosphate solubility.

## 9.0 WHITE OAK CREEK BASIN STUDY\*

### 9.1 Distribution and Transport of Radionuclides in the Bed of Former White Oak Lake (T. Lomenick)

A series of shallow auger holes, 5-6 ft deep, was completed in the bed of former White Oak Lake to define the configuration of the water table and to determine the direction of ground-water movement. Water-level measurements in these wells, made about once each week for the period Aug. 28, 1961 to Jan. 5, 1962, indicated that the depth to ground water in the area generally varies from 3 to 5 ft below the land surface during the dry summer months and from <1 to 1.5 ft during the wet winter months when transpiration and evaporation are lower.

Water-contour maps of the area show that the general direction of ground-water movement is normal to the flow of White Oak Creek in the lower portion of the site; in the upper bed the pattern is more complex. A water table contour map for Sept. 22, 1961 (Fig. 9.1) indicates that the configuration of the water table in the upper part of the area is measurably affected by the flow of surface water onto the lake bed from two streams that drain the waste pit area. During the dry summer months, these streams recharge the ground water in the lake bed, with little or no surface water flowing directly into the creek. However, in the wet winter months, when the ground water in the lake bed is close to the land surface, some of the water from these streams flows over the surface of the bed into White Oak Creek.

These two streams transport several thousand curies of Ru-106 per year from the waste pits; however, less than half the ruthenium finds its way into White Oak Creek. It is likely that much less Ru-106 enters the creek than leaves the waste pit area during the dry seasons, as the activity must be transported by ground water through the lake bed subsoil to the creek. In wet seasons, it is assumed that the input of Ru-106 to the creek more nearly approaches the output from the waste pit area because of transport of activity by surface water over the lake-bed to White Oak Creek.

A series of core samples taken in this area are being radiochemically analyzed to determine the distribution of Ru-106 in the soil.

### 9.2 Geologic and Hydrologic Studies (R. M. Richardson\*\* and W. M. McMaster\*\*)

On December 15, William M. McMaster, geologist, was reassigned to the Oak Ridge Subdistrict Office of the Surface Water Branch of the U. S. Geological Survey to investigate in greater detail the geology and hydrology of White Oak Creek Basin.

\*This project, entitled, "Environmental Radiation Studies: Evaluation of Fission Product Distribution and Movement in White Oak Creek Drainage Basin" (AEC Activity No. 060501000), is supported by the U. S. Atomic Energy Commission's Division of Biology and Medicine. All other projects covered in this Bimonthly Progress Report are supported by the Division of Reactor Development (AEC Activity No. 040405021).

\*\*On loan from Tennessee District, Surface Water Branch, Water Resources Division, U. S. Geological Survey.

The purpose of the investigation is to obtain a better knowledge and understanding of the way in which water moves through the basin. This is important in the management of radioactivity in the basin, as water is the principal agent that transports radioactive materials out of the basin into the uncontrolled environment.

A proof of a geologic map of the Oak Ridge Reservation was revised and transmitted to TVA for reproduction. An inventory of existing wells in the basin was made as a preliminary to establishing an observation well program in the basin. A reconnaissance of White Oak Creek and its tributaries to determine the location of outfalls contributing liquid wastes to the stream system was started.



## 10.0 REFERENCES

1. "Waste Treatment and Disposal Progress Report for April and May 1961," ORNL-CF-61-7-3.
2. Ibid. for October, November 1961.
3. Ibid. for August, September 1961.
4. "Chemical Technology Division Annual Prog. Report for Aug. 31, 1960," ORNL-2993.
5. J. J. Perona and M. E. Whatley, "Calculation of Temperature Rise in Deeply Buried Radioactive Cylinders," ORNL-2812 (Feb. 3, 1960).
6. H. W. Godbee and J. T. Roberts, "Survey on the Measurement of Thermal Conductivity of Solids Produced by Evaporation and Calcination of Simulated Fuel Reprocessing Solutions," ORNL-2769 (Aug. 10, 1959).
7. W. D. Kingery and F. H. Norton, "The Measurement of Thermal Conductivity of Refractory Materials," NYO-6447 (January 1955).
8. J. T. Roberts and R. R. Holcomb, "A Phenolic Resin Ion-Exchange Process for Decontaminating Low-Radioactivity-Level Process Water Wastes," ORNL-3036 (May 22, 1961).
9. R. R. Holcomb and J. T. Roberts, "Low-Level Waste Treatment by Ion-Exchange. II Use of a Weak Acid, Carboxylic-Phenolic Ion-Exchange Resin," ORNL-TM-5 (Sept. 25, 1961).
10. Op. cit, June and July, 1961, ORNL-TM-15, p. 26.
11. W. H. McAdams, Heat Transmission, Third Ed., McGraw-Hill Book Company, Inc., 1954, p. 181.
12. U. S. Geological Survey, Water Resources Division, Annual Report on Current Investigations (in preparation).
13. W. J. Kaufman, University of California, private communication, Dec. 28, 1961.
14. R. H. Merrill, "Static Stress Determinations in Salt-Site Cowboy," USBM-Report APRL 38-3.1 (1960).
15. "Effect of Accidental Spillage of Radioactive Waste into Clinch River, Rpt. No. 1, Time of Travel, Probable Flows, and Dispersion," Hydraulic Data Branch, TVA, Knoxville, Nov. 10, 1952.

16. M. A. Churchill, Health and Safety Division, TVA, private communication, January 1962.
17. L. L. Ames, "The Removal of the Bone-Seeking Group of Radioisotopes from Solution by a Calcite-Phosphate Reaction," HW-60412 (June 1, 1959).
18. Handbook of Chemistry and Physics, 37th ed., Chemical Rubber Co., Cleveland, Ohio.

### INTERNAL DISTRIBUTION

- |  |                                 |
|--|---------------------------------|
| 1. ORNL - Y-12 Technical Library<br>Document Reference Section | 34. C. W. Hancher               |
| 2-4. Central Research Library                                  | 35. R. F. Hibbs                 |
| 5-14. Laboratory Records Department                            | 36. R. R. Holcomb               |
| 15. Laboratory Records, ORNL R. C.                             | 37. J. M. Holmes                |
| 16-17. R. E. Blanco  | 38. D. G. Jacobs                |
| 18. J. O. Blomeke  | 39. W. H. Jordan                |
| 19. W. J. Boegly, Jr.  | 40. H. Kubota                   |
| 20. R. L. Bradshaw   | 41. T. F. Lomenick              |
| 21. J. C. Bresee   | 42. K. Z. Morgan                |
| 22. F. N. Browder  | 43. R. J. Morton                |
| 23. K. B. Brown  | 44. E. L. Nicholson             |
| 24. P. H. Carrigan   | 45. F. L. Parker                |
| 25. W. E. Clark  | 46. J. J. Perona                |
| 26. K. E. Cowser   | 47. R. M. Richardson            |
| 27. F. L. Culler   | 48. J. T. Roberts, IAEA, Vienna |
| 28. W. de Laguna   | 49-50. E. G. Struxness          |
| 29. F. M. Empson   | 51. J. C. Suddath               |
| 30. D. E. Ferguson   | 52. J. A. Swartout              |
| 31. H. W. Godbee   | 53. T. Tamura                   |
| 32. H. E. Goeller  | 54. J. W. Ullmann               |
| 33. J. M. Googin   | 55. M. E. Whatley               |

### EXTERNAL DISTRIBUTION

56. E. L. Anderson, AEC, Washington
57. W. G. Belter, AEC, Washington
58. W. H. Regan, AEC, Washington
59. J. A. Buckham, Phillips Petroleum Company
60. H. J. Carey, Jr., Carey Salt Company, Hutchinson, Kansas
61. C. W. Christenson, Los Alamos Scientific Laboratory
62. V. R. Cooper, AEC, Washington
63. E. F. Gloyna, University of Texas, Austin
64. L. P. Hatch, Brookhaven National Laboratory
65. W. B. Heroy, Sr., Geotechnical Corp., Dallas, Texas
66. H. H. Hess, Chairman, Earth Science Division, Commission on Ground Disposal of Radioactive Waste, Princeton University, Princeton, N. J.
67. O. F. Hill, Hanford
68. J. R. Horan, AEC, Idaho
69. J. H. Horton, Stanford Research Institute
70. E. R. Irish, Hanford
71. A. A. Jonke, Argonne National Laboratory
72. K. K. Kennedy, Phillips Petroleum Company
73. W. J. Kaufman, University of California, Berkeley

74. S. Lawroski, Argonne National Laboratory
75. B. M. Legler, Phillips Petroleum Company
76. J. A. Lieberman, AEC, Washington
77. J. A. McBride, Phillips Petroleum Company
78. R. L. Moore, Hanford
79. J. W. Morris, du Pont, Savannah River
80. R. L. Nace, Water Resources Division USGS, Washington, NAS-NRC
81. C. M. Patterson, du Pont, Savannah River
82. A. M. Platt, Hanford
83. W. H. Reas, Hanford
84. C. S. Shoup, AEC, ORO
85. L. Silverman, Harvard Graduate School of Public Health
86. J. I. Stevens, Phillips Petroleum Company
87. C. M. Slansky, Phillips Petroleum Company
88. V. R. Thayer, du Pont, Wilmington
89. Abel Wolman, Chairman, National Academy of Sciences, Committee on Waste Disposal, Johns Hopkins
90. H. M. Roth, ORO
91. J. C. Frye, State Geological Survey Div., Urbana, Ill.
- 92-106. DTIE